ROLE OF CERL2 IN THE MODULATION OF NODAL AND WNT/B-CATENIN PATHWAYS IN MOUSE EMBRYONIC STEM CELLS TO STUDY CARDIOMYOCYTE DIFFERENTIATION

MARIANA SIMAS FARIA

A dissertation submitted in partial fulfillment of the requirements for the Degree of Masters in Biomedical Research

Dissertação para obtenção do grau de Mestre em Investigação Biomédica

at Faculdade de Ciências Médicas | NOVA Medical School of NOVA University Lisbon

September, 2019

ROLE OF CERL2 IN THE MODULATION OF NODAL AND WNT/B-CATENIN PATHWAYS IN MOUSE EMBRYONIC STEM CELLS TO STUDY CARDIOMYOCYTE DIFFERENTIATION

Mariana Simas Faria

Supervisor: Prof. Dr. José António H. Belo, Stem Cells and Development, Chronic Diseases Research Center (CEDOC), Faculdade de Ciências Médicas da Universidade Nova de Lisboa

Supervisor: Dr. José Café Inácio, Stem Cells and Development, Chronic Diseases Research Center (CEDOC), Faculdade de Ciências Médicas da Universidade Nova de Lisboa

A dissertation submitted in partial fulfillment of the requirements for the Degree of Masters in Biomedical Research

Dissertação para obtenção do grau de Mestre em Investigação Biomédica

September, 2019

“Somewhere, something incredible is waiting to be known.”
Carl Sagan

ACKNOWLEDGEMENTS

My academic path started in a very different area so the decision to join a biomedical research master was personally and academically challenging and I have to thank Professor Paulo Pereira for the opportunity to join the Biomedical Research Master degree.

Most importantly, I will be forever thankful to Professor José Belo for letting me learn about regenerative medicine and allowing me to develop this fantastic and defiant project in his lab. I would also like to thank José Inácio for supervising and teaching me the experimental procedures while being patient when I was mentally confusing and possibly showing some lack of knowledge, but I have to thank him specially for being restless in helping me at the end of my thesis journey.

To the other members of the lab: Oriol Bover, Ricardo Lobo, Fernando Bonet, Sara Marques and Graça Rosas thanks for receiving me so well and being so helpful every time I needed. A special thanks to João Von Gilsa that accompanied me on the beginning of my lab work, I know it was frustrating and stressful sometimes but we managed. To Fernando Cristo and Daniela Barroso, I cannot express how deeply thankful I am for all the help and advices that you gave me, you both were so much more than lab colleagues, you become true friends. Fernando Cristo you know you were my rock during this year and I could not have made it without you, thank you for being who you are.

I am also thankful for all support from my master's colleagues. I learned a lot from you and wish you all the best!

Well, this would not be my honest acknowledgements if I did not thank my dog, so a big hug for him for never leaving my side. I would also like to thank Andreia Pereira for helping me with my dog when I was too busy to take care of him and for all the patience with him.

I am especially and eternally grateful to my parents and my grandmother for all the support during these years, I know it was not easy to deal with my breakdowns, special being so far away, but you never stopped believing that I would achieve everything that I set my mind to. I love you all so much.

RESUMO

As doenças cardíacas são a principal causa de mortalidade e morbidade nos países desenvolvidos, representando 45% de todas as mortes na Europa a cada ano (Timmis et al., 2019). Nos embriões dos vertebrados, o coração é o primeiro órgão funcional a se formar e o seu desenvolvimento envolve uma cascata de fatores de transcrição e vias de sinalização que irão regular a diferenciação de células estaminais nos distintos tipos de células cardíacas. Foram feitos estudos para promover a diferenciação de células estaminais em cardiomiócitos, como uma abordagem de medicina regenerativa, uma vez que os cardiomiócitos de um coração adulto têm uma capacidade regenerativa extremamente baixa (Nakanishi et al., 2016).

O estabelecimento do eixo esquerdo-direito é regulado por uma expressão assimétrica de *Nodal*, controlada pelo seu inibidor, *Cerberus-Like 2* (*Cerl2*). A ausência deste gene é responsável por uma variedade de malformações, conhecidas como heterotaxia. Este tipo de malformações está também frequentemente associado a doenças cardíacas congénitas (Belo et al., 2017). O ratinho knockout do *Cerl2* apresentou uma alta taxa de mortalidade, durante o primeiro dia após o nascimento, devido a um grande aumento na espessura da parede do miocárdio do ventrículo esquerdo (Araújo et al., 2014).

Neste estudo foram utilizadas células estaminais embrionárias de ratinho WT para testar a ativação experimental das vias de sinalização Nodal e Wnt/β-catenina. Pequenas moléculas têm sido estudadas para ativar estas duas vias (Nodal e Wnt). A sinalização feita pelo Nodal ou pela Ativina é normalmente indistinguível, uma vez que ambos podem regular a transcrição sinalizando através dos mesmos recetores e efectores, indicando que a activina pode ser usada para ativar a via de sinalização do Nodal, por outro lado, o CHIRON é um potente inibidor da GSK-3, que irá parar a degradação da β-catenina, permitindo a sua translocação para o núcleo, ativando os genes alvo desta via. (Buikema et al., 2013) (Pauklin e Vallier, 2015). Usando as duas moléculas descritas anteriormente, Activina A e CHIRON as respetivas vias de sinalização (Nodal e Wnt) foram ativadas durante a diferenciação em cardiomiócitos, a partir de células estaminais de ratinho. Esta experiência serve para avaliar se o fenótipo observado, durante a diferenciação em cardiomiócitos das células KO do *Cerl2,* resulta da ativação dessas vias de sinalização, devido à falta de inibição do Cerl2. Os resultados mostraram que, embora o fenótipo das diferenciações com a ativação das duas vias (Nodal e Wnt) parecesse semelhante ao apresentado pelas células KO, não houve um aumento dos marcadores cardíacos, como observado nas diferenciações das células KO.

ABSTRACT

Heart disease is the main cause of mortality and morbidity in developed countries, accounting for 45% of all deaths in Europe, each year (Timmis et al., 2019). In vertebrate's embryos, the heart is the first functional organ to form and its formation involves a cascade of transcription factors and signaling pathways that will regulate cell fate towards distinct heart fields. This cascade of events has been included in studies that differentiate stem cells into cardiomyocytes as a regenerative medicine approach to heart failure, because cardiomyocytes rarely regenerate in post-natal hearts (Nakanishi et al., 2016).

The left-right axis establishment is regulated by an asymmetric expression of *Nodal*, controlled by its inhibitor, *Cerberus-like 2* (*Cerl2*). The absence of *Cerl2* gene is responsible for a variety of malformations comprising the left-right axis establishment, known as heterotaxia. These malformations are often associated with congenital heart diseases (Belo et al., 2017). *Cerl2* knockout mouse displayed a high mortality rate during the first day after birth due to a particularly large increase in the left ventricular myocardial wall thickness (Araújo et al., 2014).

Wild type mouse embryonic stem cells have been used, in this study, to test the effects of the experimental activation of Nodal and Wnt/β-catenin pathways. Nodal and Activin ligands can regulate transcription by signaling through the same receptors and effectors, indicating that Activin can be used to activate Nodal signaling pathway and CHIRON is a potent GSK-3 inhibitor, allowing the translocation of β-catenin to the nucleus, activating Wnt/β-catenin signaling (Buikema et al., 2013) (Pauklin & Vallier, 2015). Using the two previously described molecules, Activin A and CHIRON, the respective pathways (Nodal and Wnt) were activated during cardiomyocyte differentiation of mouse embryonic stem cells. This was performed to assess whether the phenotype of the *Cerberus-Like 2* Knock-Out during cardiomyocyte differentiation results from the activation of these signaling pathways, due to the lack of inhibition from *Cerl2*. The experiments showed that, although the phenotype of the differentiations with the activation of the two pathways (Nodal and Wnt) seemed similar to the one presented by the KO cells, there was not a significative upregulation of the cardiac markers, compared with the observed on the *Cerl2* KO differentiated cells.

CONTENTS

LIST OF TABLES

LIST OF FIGURES

ABBREVIATIONS

α-MHC	*Alpha Myosin Heavy Chain*
A-P	Anterior-Posterior
AVE	Anterior Visceral Endoderm
BMP	Bone Morphogenetic Protein
cDNA	Complementary Deoxyribonucleic Acid
Cerl2	*Cerberus-like 2*
CHD	Coronary Heart Disease
CMC	Cardiogenic Mesodermal Cells
CK1	casein kinase 1
cTnT	*Cardiac Troponin T*
DMEM	Dulbecco's Modified Eagle Medium
DMSO	Dimethyl Sulfoxide
DNA	Deoxyribonucleic Acid
dNTP	Deoxynucleotide
D-V	Dorso-Ventral
DVE	Distal Visceral Endoderm
E	Embryonic Day
EB	Embryoid Body
EGF-CFC	Epidermal Growth Factor-cripto, frl-1, cryptic
EOMES	T-box protein eomesodermin
EPI	Embryonic Epiblast
ES	Embryonic Stem
ExE	Extraembryonic Ectoderm
FBS	Fetal Bovine Serum
FGF	Fibroblast Growth Factor
FHF	First Heart Field
Fw	Forward
Gapdh	*Glyceraldehyde-3-Phosphate Dehydrogenase*
GSK3	Glycogen Synthase Kinase 3
ICM	Inner Cell Mass
IgG	Immunoglobulin G
Isl1	*Isl1 Transcription Factor, LIM Homeobox 1*
KO	Knockout
LIF	Leukemia Inhibitor Factor
LPM	Lateral Plate Mesoderm
L-R	Left-Right
LRP6	low-density lipoprotein receptor related protein 6
mRNA	Messenger RNA
Nanog	*Nanog Homebox*
NEAA	Non-Essential Amino Acids

Nkx2.5	*NK2 Homeobox 5*
Oct4	*Octamer 4*
PBS	Phosphate-Buffered Saline
PCR	Polymerase Chain Reaction
P-D	Proximal-Distal
PFA	Paraformaldehyde
Pitx2	*Paired-like Homeodomain Transcription Factor 2*
PE	Primitive Endoderm
PS	Primitive Streak
qRT-PCR	Quantitative Real-Time Polymerase Chain Reaction
RNA	Ribonucleic Acid
Rv	Reverse
SHF	Second Heart Field
SSEA-1	*Stage-Specific Embryonic Antigen-1*
TE	Trophectoderm
TEA4	TEA Domain Transcription Factor 4
TGF-β	Transforming Growth Factor β
VE	Visceral Endoderm
Wnt	Wingless/ Integrated Family Members
WT	Wild Type
YAP	Yes-associated protein 1

CHEMICAL SYMBOLS

$C_{22}H_{18}Cl_2N_8$	CHIR99021
CO2	Carbon Dioxide
KH_2PO_4	Monopotassium phosphate
NaCl	Sodium Chloride
KCl	Potassium Chloride

UNITS

%	Percentage
µg	Microgram
µg/mL	Microgram per Milliliter
µL	Microliter
µM	Micromolar
bp	Base Pair
oC	Degree Celsius
kb	Kilobase Pair
kDa	Kilodalton
mL	Milliliter
ng	Nanogram
pH	Potential of Hydrogen
rpm	Rotations per Minute Units/Microliter
v/v	Volume/ Volume

1. INTRODUCTION

Cardiovascular disease is the leading cause of morbidity and mortality in developed countries, accounting for 45% of all deaths in Europe each year (Timmis et al., 2019). It is estimated that coronary heart disease (CHD) is responsible for 7,4 million deaths, worldwide and it is expected that by 2030, 23,6 million people will die from CHD. (Chadwick, et al., 2018) The prevalence of myocardial infarction is higher in men and independent of age. Some risk factors like obesity, increased blood pressure, high cholesterol, diabetes, alcohol ingestion and cigarette smoking can contribute to the development of diseased heart. Other factors like left ventricular hypertrophy and family history of premature coronary heart disease can also be a predictor for the development of cardiovascular disease (Wilson et al., 1998).

Upon myocardial infarction, the heart tries to repair itself and return to a pre-injured state, as much as possible (with very low success rate on the adult heart), so it undergoes several stages to repair the damaged area. The inflammation process is the first one to take place, cytokines and growth factors start recruiting cells that are necessary to clean the necrotic tissue and recruit other cells that will become myofibroblasts. It has been described that surrounding fibroblasts migrate to the damaged area and undergo myofibroblast conversion. Although fibroblasts may be the main cells in this process, it has also been described that circulating fibrocytes or stem cells can also be recruited and trans-differentiate into myofibroblasts. Regardless of the source, myofibroblasts are responsible for synthetizing large amounts of extracellular matrix (ECM), necessary to scarification. (Czubryt, 2012). Distinct to wound healing, the scarification in the heart stays for the rest of the patient's life because scar tissue fails to be degraded and recellularized. As cardiomyocytes are terminally differentiated and have left the cell cycle, they are not able to repopulate the infarcted area in sufficient number to promote repair. This scar tissue can have negative influence in the cardiac function by impairing contraction and relaxation, moreover the myofibroblasts and the ECM of the scar tissue, produce electrical properties distinct from the surrounding tissue, thus contributing to arrhythmogenesis (Czubryt, 2012) (Voges et al., 2017).

Some studies have documented that neonatal mouse hearts are able to repopulate the affected area, upon myocardial infarction, therefore being able to regenerate the heart tissue, however it is still not clear if the human neonatal heart possess this ability. Voges (2017) and his colleagues, were able to create a human neonatal heart organoid, using human pluripotent stem cells (hPCS) derived cardiomyocytes and by inflicting a localized injury that would mimic a myocardial

infarction they were able to show that this organoid was able to regenerate. This study indicates that this regenerative capacity may be intrinsic to the immature human heart (Voges et al., 2017). Clinical studies regarding this regenerative capacity in the neonatal human hearts has recently emerged, like Boulton et al. (1991) that reports the case of two children who survived myocardial infarction in the early neonatal period and Haubner et al. (2016) have documented a case of a newborn child who have suffered from a severe myocardial infarction due to a coronary artery occlusion and made a full recovery, within weeks, that translated into long-term normal heart function.

Due to the lack of regenerative capability of the cardiomyocytes in post-natal hearts, people who suffer from congenital or acquired heart disease often develop chronic heart failure, which will lead to the necessity of heart transplant on the late-stage of the disease, for this is the only definitive treatment available nowadays (Nakanishi et al., 2016). Heart failure and congenital heart defects have fueled the pharmacologic industry for developing new organ-independent treatments to prevent or limit the symptoms and consequently restoring some life quality. Different groups have shown that the heart has a regeneration capacity of 1% per year and since the first reported study, in 1998, indicating that the heart was repaired using transplanted skeletal myoblast, different studies have been conducted using different types of cells like pluripotent and multipotent stem cells (Cambria, et al., 2016) (Taylor, et al., 1998). Survivability of the engrafted cells is one of the most challenging problems when it comes to cell-based therapy, to overcome this issue, Fischer (2009) and his colleagues have performed intramyocardial injections, in infarcted female mice, of cardiac progenitor cells expressing Pim-1 Kinase, a cardiac protective kinase, capable of enhancing cell survival and proliferation. With this approach they were able to show a reduction of the infarct size and increased vasculature, consistent with increased proliferation, greater levels of cellular engraftment and functional improvement. Cardiac fibroblasts are present in a large number and distributed throughout the heart, most of the population is in a state of inactivity, thus, in 2010, a group of investigators focused on this type of cells. They have reported that the combination of Gata4, Mef2c and Tbx (GMT), three developmental transcription factors, was able to effectively trans-differentiate cardiac fibroblast into cardiomyocyte-like cells, opening doors to *in vivo* differentiation, in the heart (Srivastava, 2016) (Ieda *et al*., 2010). Upon coronary artery ligation in mice, Qian (2012) and his team injected in the surrounding myocardium infarcted zone, a retroviral system expressing the three previously described transcription factors (GMT), in order to directly reprogram cardiac fibroblast into

cardiomyocyte-like cells. The results showed that more than 50% of the *in vivo* induced cardiomyocytes resembled endogenous ventricular cardiomyocytes as they assemble sarcomeres, were binucleate and expressed cardiac markers. There was also evidence of electrical coupling as they expressed connexin 43, a gap junction protein in the heart that is responsible for electrical coupling and synchronized beating of the myocytes. This cells also generated Ca^{+} transients and beating activity (Qian et al., 2012). Nonetheless, cell-based therapies have always reported high incidences of arrhythmogenesis that are yet not fully understood, so Yu (2019) and his colleagues generated a comprehensive framework for multiscale cardiac electrophysiology simulations of cell-based heart repair, with realistic therapy features represented. This program allowed them to understand that cell dosage, special distribution of the engraftment and injection location were critical to the development of arrhythmogenesis, later on. They have also correlated transdifferentiated cardiomyocytes engraftments onto Purkinje fibers with the development of conduction block and consequently heart rhythm disfunction. The contributing of this simulation program can be of great importance in the development of arrhythmia-free cell-based therapies.

Pluripotent Stem cells play a very important role as an *in vitro* model to understand the mechanisms, important pathways and key regulators of cardiomyogenesis. Therefore, many studies have made use of the ability of these cells to differentiate into different types of cells and to be able to mimic the mechanisms underlying *in vivo* embryogenesis, to understand cardiomyogenesis complexity (Leitolis et al., 2019). Therefore, *Cerberus-Like 2* (*Cerl2*) has been implied as an important player for the establishment of left-right asymmetry of the organs and also for the correct development of the organs, particularly, the heart (Marques et al., 2004). This gene acts as a Nodal inhibitor, a key regulator of the left-right axis and defects in Cerl2 can lead to laterality defects known as heterotaxia, in addition to congenital heart defects. A study with *Cerl2* knockout mice has associated the absence of this gene with specific heart defects like hyperplasia and systolic dysfunction. It was possible to identify a particularly large increase in the left ventricular myocardial wall thickness, due to a higher mitotic index. (Belo, Marques, & Inácio, 2017) (Araújo, Marques & Belo, 2014). Defects on *DAND5*, the *Cerl2* human homolog, have also been associated in such defects. A study has identified two patients with a missense mutation in *DAND5*, one of them suffered from left isomerism, atrial septal defect and pulmonary atresia and the other displayed Tetralogy of Fallot and pulmonary atresia (Cristo, et al., 2017). Preliminary data shows that Wnt/β-Catenin signaling levels were higher in the compact myocardium of the KO embryos, suggesting that *Cerl2* may also have an inhibitory role in this pathway. Both TGF-β/Nodal

and Wnt/β-Catenin signaling pathways have been described as important participants in the heart development, as they are able to influence cardiac differentiation and proliferation (Cai et al., 2012) (Buikema et al., 2013). Considering everything, it is reasonable to hypothesize that *Cerl2* regulates both signaling pathways in mice heart and possibly modulates cardiomyocytes proliferation and is involved in the decision mechanism of the originated cells, explaining the phenotype observed in the *Cerl2*$^{-/-}$ mouse embryos.

1.1. Aims of the project

When differentiated into cardiomyocytes, the *Cerl2* KO cells exhibit a peculiar phenotype that can be linked to the phenotype observed *in vivo*, on the neonatal mice hearts. These hearts presented an increase in the thickness of the left ventricle myocardium wall, related to an upregulation of the Nodal signaling pathway (Araújo, et al., 20014). Unpublished work performed in the lab reported an upregulation of Wnt/β-Catenin signaling pathway, another important pathway for the heart development. For this dissertation, the final aim is to assess whether the phenotype of the *Cerberus-Like 2* KO during cardiomyocyte differentiation results from the activation of these signaling pathways, due to the lack of inhibition from *Cerl2*. For this assessment the following steps were performed:

I. Characterize the activation profile of TGF-β/Nodal and Wnt/β-Catenin signaling pathways during cardiomyocyte differentiation in WT and *Cerl2* KO cells.
II. Single and co-activation of TGF-β/Nodal and Wnt/β-Catenin signaling pathways, in the WT cells, using Activin A and CHIR99021.
III. Study the obtained phenotype to see if it is similar to the one acquired by the KO-derived cardyomyocytes.

2. BACKGROUND

2.1. Early Mouse Development

The embryo development starts at conception or fertilization, upon a fusion of a male spermatozoid and a female oocyte, that will form the zygote. The fertilized egg will then start a series of sequential divisions into progressively smaller cells, the blastomeres. This will form a blastocyst that consists in a hollow ball of cells, that will be implanted into the maternal uterine wall and give rise to embryonic and extraembryonic tissue during development. The blastocyst development starts with two major waves of asymmetric division, structuring a morula. This process is important for cell fate decision, as cell positioning within the embryo and cell polarity along the apicobasal axis will be decisive for early cell commitment. Recent studies have shown that Hippo signaling is important for cell fate decision. At this point of differentiation activation and inactivation of this pathway in the inner and outer cells will further promote cell fate and help organize the blastocyst, that will be constituted by a pluripotent inner cell mass (ICM), surrounded by trophectoderm (TE). Upon fusion with the uterine wall, the blastocyst will be in its later stage, presenting a higher level of differentiated cells and, by this time, the blastocyst comprises the extraembryonic trophectoderm, the primitive endoderm (PE) and the embryonic epiblast (EPI) (Bedzhov et al., 2014) (Sasaki, 2015).

Trophectoderm is the first cell lineage to be differentiated in the mouse embryo and will give rise to the placenta, a structure exclusive to the mammalian development. It is thought that TE is formed in the absence of Oct4, but its commitment towards TE, starts before Oct4 downregulation, suggesting that some positive factors are also involved. Studies have revealed the importance of Cdx2 in TE specification, as this transcription factor is required for Oct4/Nanog repression and normal blastocyst development. This transcription factor has also been implied in the generation of proper trophoblast stem cells and its vital for their self-renewal. However, Cdx2 alone it's not fundamental for TE commitment, as these cells can be induced by over expression of EOMES, meaning that they can have some overlapping effect in TE induction. Furthermore, some evidences suggested that EOMES may be a target of Cdx2 (Strumpf, 2005) (Niwa et al., 2005). Nishioka (2009) and his colleagues have reported that differential expression of Cdx2 in inner and outer cells is promoted by the modulation of Tead4 and coactivator protein Yap, that it's localized in the nuclei of inner and outer cells of the morula. Yap is phosphorylated in the inner cells,

inactivating Tead4, whereas it is active on the outer cells, thus promoting the expression of Cdx2 in these cells, that will lead to Oct4 downregulation and TE specification.

Inner cell mass is the precursor of PE and EPI and commitment to this cell lineage has been attributed to the function of two transcription factors, Oct4 and Nanog. Some studies have revealed that *Oct4* null embryos fail to acquire the ICM lineage specific identity, leading to a disruption in the development of PE and EPI (Le Bin et al., 2014). Cell commitment within ICM has been attributed to several factors as cell sorting, possibly achieved by multiple cell behaviors like actin-dependent active cell movements that will dictate the position of PE committed cells, as well as cell apoptosis for cells who failed cell sorting. Activation and inactivation of certain genes can also be implied in the specification of PE and EPI and some evidences support a link between GATA6, SOX17, GATA4 and SOX7 transcription factors activation and PE commitment (Artus, Piliszek, & Hadjantonakis, 2011). Nevertheless, PE cells present a loss of plasticity compared to EPI cells that stay more pluripotent. This loss of plasticity in the PE cells is due to an exclusion of the pluripotency marker Oct4. However, precursors of EPI exhibit less plasticity than the precursors of PE, possibly due to extracellular cues that have effect only on the EPI precursors, thus ensuring the formation and preservation of the pluripotent fetal lineage (Grabarek et al., 2011).

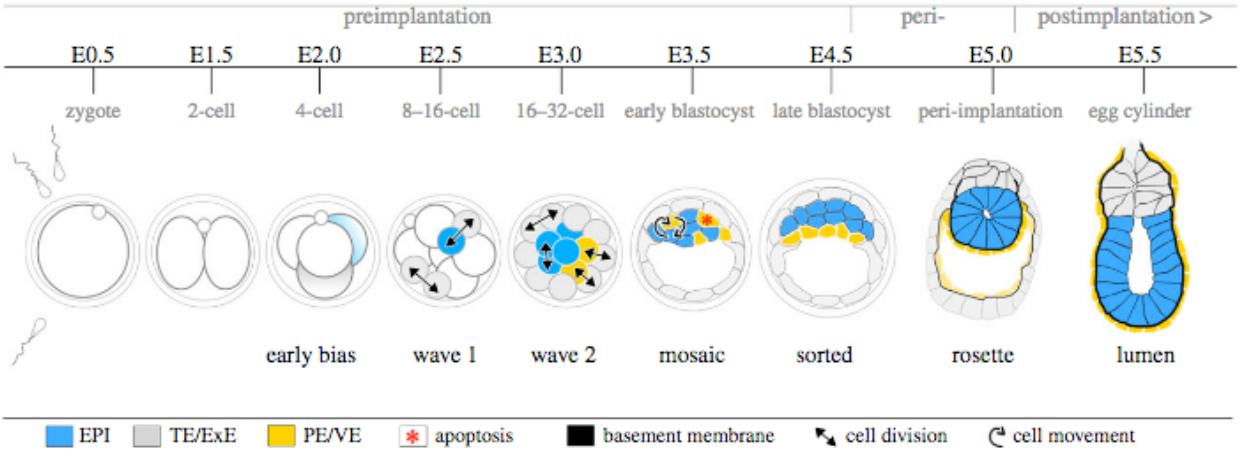

Figure 1 - ***Overview of early mouse development.***
The zygote consists in a totipotent cell capable of subsequently dividing in smaller cells called blastomeres, until the morula stage its reached. At E3.5, the blastocyst is composed by two different cell lineages: the inner cell mass (ICM) and the trophectoderm (TE). Ultimately, the ICM is responsible for the embryo formation (Adapted from Bedzhov et al., 2014)

2.2. Patterning the Embryo

The body axis of a mammalian embryo only starts to become morphologically visible several days after implantation, moreover, the anterior-posterior axis can only be unequivocally identified right before gastrulation starts. For this reason, it was generally believed that the cells within the early

embryo were all in a naïve state and their fate was decided through interactions between each other, rather than by developmental cues. Now we know that patterning cues arise before the morphological changes are evident. Polarity, asymmetric gene expression and programmed distribution of other morphogenic determinants are essential for the embryo patterning, yet, owing to its plasticity, the embryo is capable of recovery from experimental perturbation that would disrupt the embryo patterning (Chan et al., 2002).

2.2.1. Anterior-Posterior and Dorso-Ventral Axes establishment

The Anterior-Posterior (A-P) axis establishment begins upon implantation of the embryo in the uterine wall, around day (E)4.5. Right after implantation, the embryo suffers a burst of proliferation that will induce a structural change from the bowl-like shape to an elongated egg-cylinder structure, that will be the foundation of the future body. This transformation will lead to changes in shape and topology of the embryo tissues, as a result, the epiblast will become positioned at the distal part of the egg-cylinder structure, whereas the trophectoderm-derived extraembryonic endoderm (ExE) locates at the proximal part and both of these tissues are surrounded by primitive endoderm-derived visceral endoderm (VE). At this point, distal visceral endoderm (DVE) emerges at the distal part of the embryo, which will further establish the A-P axis polarity, along the proximal-distal (P-D) orientation of the embryo. Elongation of the embryo, its P-D orientation and a combination of inductive signaling like TGF-β family members, Nodal and Activin, seem to be crucial for the development of DVE. Thereafter, DVE will expand and undertake unilateral movement towards the prospective anterior side, by E6.0, thus stipulating where the head will form (Morris et al., 2012) (Matsuo & Hiramatsu, 2017). The DVE movement towards the prospective anterior side of the embryo is fundamental for the anterior visceral endoderm formation (AVE), that will locally suppress the primitive streak (PS) and induce the formation of anterior ectoderm (Shioi et al., 2017). Thereupon, PS will start emerging at the posterior side of the epiblast, a fundamental process for the formation of the three germ layers – ectoderm, mesoderm and endoderm – necessary for the development of all types of tissues and also to further establish the three-dimensional body plan (Williams et al., 2011). The PS will give rise to the node that will form the axial mesendoderm along the midline, also defining the cells that will populate this area – prechordal plate and notochord. This event is essential for the dorso-ventral (DV) axis establishment because it will define the group of cells that will arise in each side of the axis, so endoderm will mark the ventral side and ectoderm the dorsal side (Beddington & Robertson, 1999).

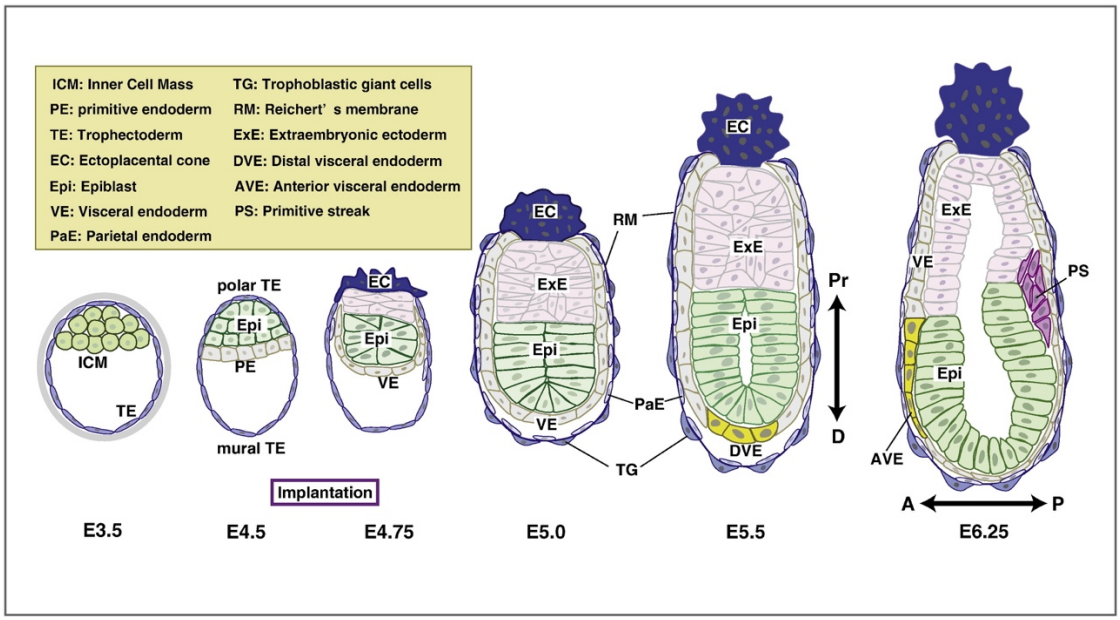

Figure 2 - ***Establishment of the Anterior-posterior axis and emergence of the primitive streak.***
The diagram shows the DVE formation, expansion and unilateral migration towards the prospective anterior side, giving rise to the AVE, at E6.25. (Adapted from Bedzhov et al., 2014)

2.2.2. Left-Right Axis establishment

A correct left-right (L-R) determination is crucial for the morphogenesis and correct placement of visceral organs (Hamada et al., 2002). The process for the L-R establishment can be divided into several steps, first there is a break of symmetry at the Node, a structure located at the anterior part of the primitive streak (Nonaka et al., 2002) (Davidson & Tam, 2000). This break of symmetry is due to a leftward fluid flow at the node, generated by motile cilia, that will target Cerberus-like 2 (Cerl2) an important Nodal inhibitor. Moreover, this will promote an asymmetric expression of Cerl2 by decay of its mRNA on the left side of the perinodal crown cells of the mouse embryo (Nakamura et al., 2012). Thus, Cerl2 expression will be higher on the right side of the node, inhibiting Nodal that will be active on the left side. Afterwards, nodal signaling cascade is activated on the left lateral plate mesoderm (LPM), by the nodal present inside the node (Marques et al., 2004) (Oki et al., 2007). Even though this mechanism is important for L-R establishment, it is insufficient to determine the *embryonic situs*. Therefore, once the Nodal is active on the left LPM it requires a self-enhancement and lateral-inhibition system, promoted by *Nodal* and *Lefty* genes expression. An activator and a feedback inhibitor, respectively, that will expand the nodal signaling along the AP axis and also ensure the presence of Nodal in the correct time and place. (Nakamura et al., 2006). Finally, the situs-specific organogenesis takes place, for this process *Pitx2* has been identified as a main player, but not the only one. Nodal will activate *Pitx2*, that will also be express asymmetrically in the left LPM and its expression is maintained by *Nkx2* until much later stages than does Nodal and *Lefty*. *Pitx2* expressing cells will develop left-side morphologies, so in the

absence of this gene, bilateral organs (e.g. lungs) will exhibit right isomerism but some laterality events do not seem to be affect by the absence of *Pitx2*, meaning that there are other key players yet to be discovered (Shiratori & Hamada, 2006).

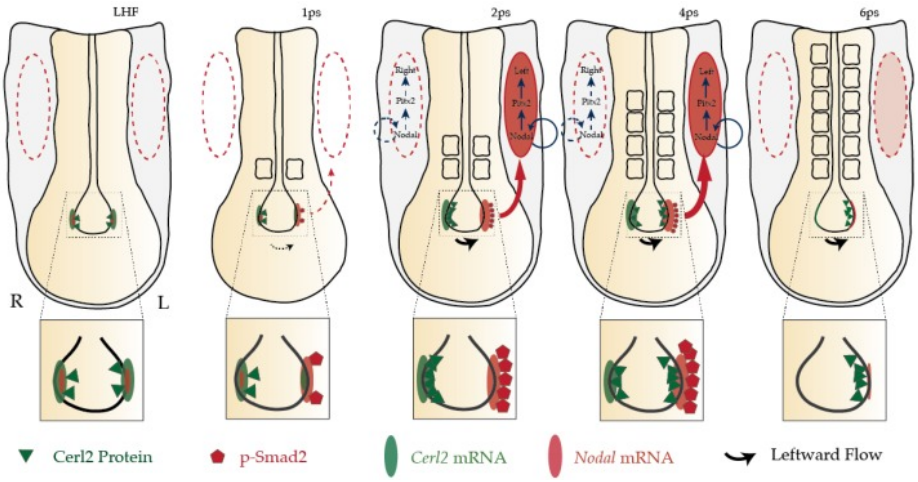

Figure 3 - ***The role of Cerl2 and Nodal in the Left-Right axis establishment****.*
As soon as the cilia at the node began to rotate generating a weak leftward flow, the asymmetric expression of *Cerl2* is established. This local reduction of *Cerl2* mRNA (and Cerl2 protein) in the perinodal cells on the left side of the node results in an increase of active Nodal signal that is later translocated to the LPM (Adapted from Belo et al., 2017).

2.3. Cerberus Family

The *Cerberus-Like* family is structurally related to the cysteine-knot superfamily, comprising a group of small secreted proteins (from 185 a.a. Cerl2 to 272 a.a. Xcer1 and Cerl1) that behave not only as an antagonist of members from the TGF-β family, such as BMP and Nodal, but also as an antagonist of Wnt. These secreted proteins are composed by a signal peptide at the N-Terminal and nine cysteines at the C-Terminal, creating a Cystein-Rich Domain (Belo et al., 2009) (Piccolo et al., 1999).

Cerberus was first described in the Xenopus model as a protein expressed in the yolky endomesodermal cells placed in the deep layer of Spemann-Mangold organizer. Microinjections of *Cerberus* mRNA in the Xenopus blastomeres have led to the formation of ectopic heads and duplication of some internal organs, such as the heart and liver (Bouwmeester et al., 1996). *Cerberus* homologues have been described in other species like *Cerl1* and *Cerl2* in mouse, *cCer* in chicken, *zCharon* in zebrafish and *Dand5* in humans.

2.3.1. *Cerberus-Like 2*

Cerberus-Like 2 (*Cerl2*) is a small secreted protein (approximately 20-kDa), member of the Cerberus/Dan family. As an antagonist of the TGF-β/Nodal signaling, *Cerl2* has an important role in breaking the L-R symmetry in the node and in the transmission of the L-R asymmetry to the LPM, during the mouse gastrulation (Belo, Marques & Inácio, 2017). Studies have shown that *Cerl2*

directly binds to Nodal and owing to its small size, the Cerl2 protein is capable of generating a fluid-dependent stationary gradient, that will lead to its accumulation on the left side of the mouse node (Marques et al., 2004) (Inácio et al., 2013). Inácio (2013) and his colleagues demonstrated that Cerl2 co-localizes with Nodal and is located in the perinodal crown cells. Interestingly, at 3-somite stage, Cerl2 protein was present in both sides of the node, contrasting to its gene expression, only on the right side of the mouse node. The right-side expression of *Cerl2* is dynamically transposed to the left side of the node at 3-4 somite stage and it's extinct at this location after 6-somite stage. Inácio (2013) and the team have also validated that both expression and localization of Cerl2 protein is dependent of the fluid flow inside the mouse node.

2.4. Embryonic Origins of the Mouse Heart

In vertebrates, the heart is the first organ to develop and function and it's a complex process that starts with gastrulation. Upon gastrulation, mesodermal tissues, responsible for the heart formation, become evident (Moorman et al., 2003). Cardiac mesoderm progenitors arise from the PS and move anterior-laterally towards the splanchnic mesoderm, located in the LPM area, to form the heart crescent, a primitive heart structure that will be fully formed at E7.5. (Savolainen, Foley, & Elmore, 2009) (Vincent & Buckingham, 2010). Studies with mice lacking MesP1 and MesP2 fail to induce the migration of cardiac mesoderm precursors from the primitive streak, impairing the development of cardiac tissue and other mesodermal structures, attesting the fundamental role of these transcription factors in the early cardiac development (Bruneau, 2002). Two major waves of cell migration have been described, the first one being the cells that migrate from the PS to form the cardiac crescent, also known as first heart field (FHF) and then there is a second migration wave of cells, from pharyngeal mesoderm towards the medial anterior part of the heart crescent, to form the second heart field (SHF) (Xin, Olson, & Bassel-Duby, 2013). FHF cells will express non-canonical Wnt, BMP2 and FGF8 while SHF cells will express canonical Wnt, Sonic Hedghog (SHH) and FGFs (Galdos et al., 2017). Afterwards, at E8, the cardiac crescent fuses across the ventral midline, to create a single beating tube mostly derived from the FHF, the SHF will contribute for expansion of this structure by providing undifferentiated cardiac precursors at the anterior and posterior region, also contributing to formation of arterial and venous poles (Ivanovitch, Esteban, & Torres, 2017) (Xin, Olson, & Bassel-Duby, 2013). At this point, the tube is composed by an outer myocardial cell layer and an inner endothelial cell layer. At E8, the contractions in the heart tube are still irregular but a regular heart beat will be established by E9 (Savolainen, Foley, & Elmore, 2009). Subsequently, the heart tube will undergo a rightward

looping, at E8, that will lead to the development of primitive ventricles and atria. Consequently, the venous pole will move anteriorly, acquiring the correct position for the future cardiac chambers develop properly (E10) (Xin, Olson, & Bassel-Duby, 2013). Finally, FHF will generate the myocardium of the left ventricle, part of the right ventricle and part of the atria and the SHF will give rise to the myocardium of the right ventricle, cardiac outflow tract, and part of the left ventricle and atria (Lin et al., 2012). From E9.5 several structures are already distinguishable, such as, the aortic sac, the bulboventricular canal (primitive right ventricle), the primitive left ventricle, the outflow track, the common atrial chamber and the atrioventricular canal. The correct late development of the heart (from E10.5 until E15) will depend on the ballooning of the chambers, septation of the atrial and ventricular chambers and separation of the atrioventricular canal. That will lead to the formation of the mitral and tricuspid orifices and later the formation the respective valves (Savolainen, Foley, & Elmore, 2009) (Lin et al., 2012).

Besides the cells important for the FHF and SHF formation, other population of cells also contribute to the correct formation of the heart, such as the proepicardial organ, that is a mesenchymal transitory structure located at the posterior end of the heart tube. This structure is responsible for providing cells that will grow over the myocardium of the heart tube, configuring the outer layer of epicardium. Some of the epicardial cells can enter the heart tube, by suffering an epithelial to mesenchymal transition, thus contributing not only for the formation of smooth muscle and coronary blood vessels, but also compose the population of cardiac fibroblast and interstitial cells (Vincent & Buckingham, 2010).

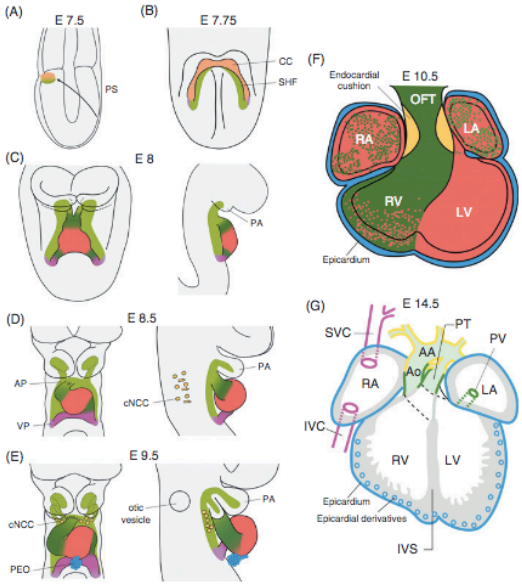

Figure 4 - ***Embryonic heart development***. The diagram shows the development of the FHF and SHF. The FHF progenitors will give rise to left ventricle (LV) and atria while SHF progenitors are involved in derivation of the outflow tract (OFT), right ventricle (RV) and atria. (Adapted from Vincent & Buckingham, 2010)

2.5. Pathways involved in heart formation

The heart development in mouse is orchestrated by a well-organized network of different pathways and their respective activation and inhibition, at certain developmental time windows, is the key for a correct formation of the heart. Two important pathways, Nodal signaling and Wnt signaling, will be described in this thesis, due to their importance in heart development, as well as, their associations with the *Cerl2* gene.

2.5.1. Nodal Signaling

Nodal is a member of the Transforming Growth Factor type β (TGF-β) superfamily of morphogens and it has been implied as a key player in the embryo development, responsible for gastrulation, germ layer formation and patterning, specifically important for the axes formation. Thus, the multiple functions of Nodal in cell fate specification will depend on concentration and exposure (Guzman-Ayala et al., 2009). Studies have shown that Nodal is not only necessary for maintenance of pluripotency at the epiblast stage, of mouse embryonic stem cells, but also for extraembryonic tissue differentiation (Pauklin & Vallier, 2015). Nodal signaling is essential for mesoderm and endoderm induction, Conlon et al. (1994), described that *Nodal* null mice embryos failed to generate a distinct primitive streak and presented a sporadic development of some anterior mesoderm, randomly positioned. Moreover, several studies have reported that cardiac induction requires signaling generated by endoderm that will activate TGF and Nodal pathways (Samuel & Latinkić, 2009).

In order to activate it signaling, Nodal interacts with membrane serine/threonine kinases (type I and type II receptors) (Guzman-Ayala et al., 2009). Firstly, Nodal binds to the type II activin receptors that will trigger the recruitment, phosphorylation and activation of type I activin receptors, inducing the phosphorylation of the Smad transcription factors (Pauklin & Vallier, 2015). Nodal signaling requires EGF-CFC family of co-receptors, which are small extracellular proteins comprising cysteine-rich domain, to attain specification for the type I receptor ALK4 (Shen, 2007). When Smad2/3 are phosphorylated, they are able to interact with Smad4, subsequently forming a transcriptional complex that moves into the nucleus. Smad2 and Smad4 bind directly to DNA, by recognizing a Smad-binding element (Pauklin & Vallier, 2015). This transcriptional complex, in association with FoxH1 transcription factor, will lead to the expression of some downstream Nodal target genes, such as, *Lefty1/2* and *Pitx2* (Shen, 2007). Nodal signaling is regulated by multiple mechanisms like the extracellular antagonists *Lefty1/2* and Nodal and agonists *CRIPTO1* (Pauklin & Vallier, 2015).

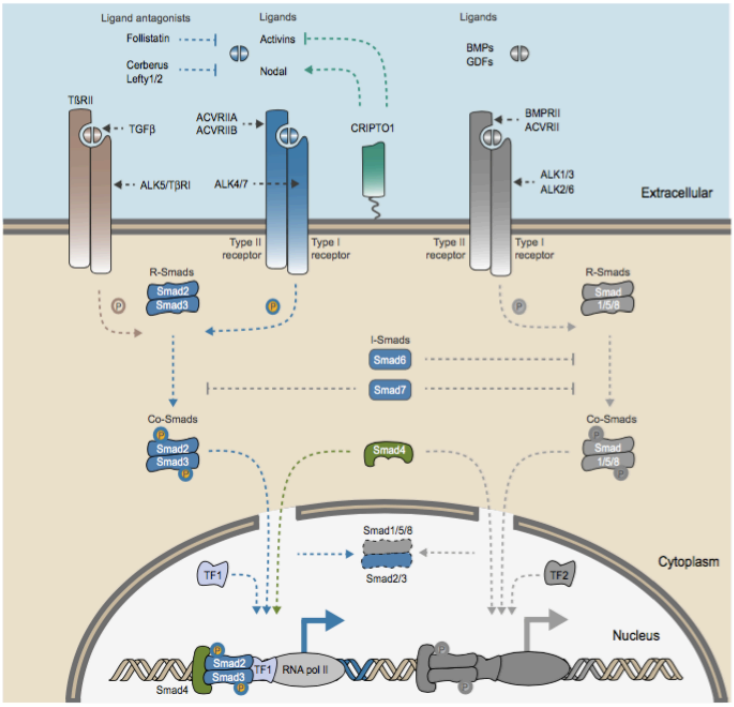

Figure 5 - ***Nodal Signaling.***
Nodal binds to ALK4 receptor leading to the phosphorylation of Smad2. ρ-Smad2 binds to Smad4 forming a complex that will translocate into the nucleus and subsequently activate the Nodal pathway target genes (Adapted from Pauklin & Vallier, 2015).

2.5.2. Wnt Signaling

Wnt signaling is an ancient and evolutionary conserved pathway, comprising a family of secreted glycoproteins responsible for the regulation of a wide variety of biological processes, including cell fate determination, cell proliferation, cell migration, cell polarity, patterning and organogenesis, during embryonic development (Komiya & Habas, 2008). This signaling is expressed in a temporospatial manner during embryonic growth, in order to induce several crucial events for the embryo development, being highly specific in mesoderm induction and cardiac fate determination (Flaherty, Kamerzell, & Dawn, 2012). Studies where Wnt signaling was disrupted showed and absence of the primitive streak and consequently a failure in mesoderm induction and node formation (Buikema et al., 2013). Both canonical and non-canonical Wnt pathways are necessary for a correct heart development. Canonical Wnt pathway is crucial for the early stages of cardiac commitment and development, whereas non-canonical Wnt pathway has been linked to the subsequent cardiac specification (Mehta et al., 2014). Wnt/β-Catenin pathway and specifically important for the development of the SHF, but it's also crucial for controlling the ventricular myocyte proliferation during the development and perinatal stages (Buikema et al., 2013) (Fan et al., 2018).

For the correct expression of the Wnt/β-Catenin pathway, Wnt binds to a receptor, the seven-pass transmembrane frizzled receptor and also to its co-receptor, the low-density lipoprotein receptor

related protein 5/6 (LRP5/6). The formation of this complex will recruit the scaffolding protein dishevelled, resulting in the phosphorylation of the LRP6 co-receptor, thus inducing the activation and recruitment of the Axin complex, comprising several compounds, among them, the casein kinase 1 (CK1), and glycogen synthase kinase 3 (GSK3). This recruitment will stop the Axin complex-mediated phosphorylation of β-Catenin pathway, leading to an accumulation of this protein and posterior translocation into the nucleus, where it will form a complex with TCF/LEF and then activating the Wnt target gene expression. When Wnt pathway is not active, the Axin complex is constantly phosphorylating β-Catenin. The sequential phosphorylation of the amino terminal of β-Catenin, performed by CSK1 and GSK3, will induce the recognition of β-Catenin by an E3 ubiquitin ligase subunit, thus provoking the ubiquitination of this protein by the proteasome. This constant degradation of β-Catenin will prevent its accumulation and further translocation to the nucleus, stopping Wnt target gene expression (MacDonald, Tamai, & He, 2009).

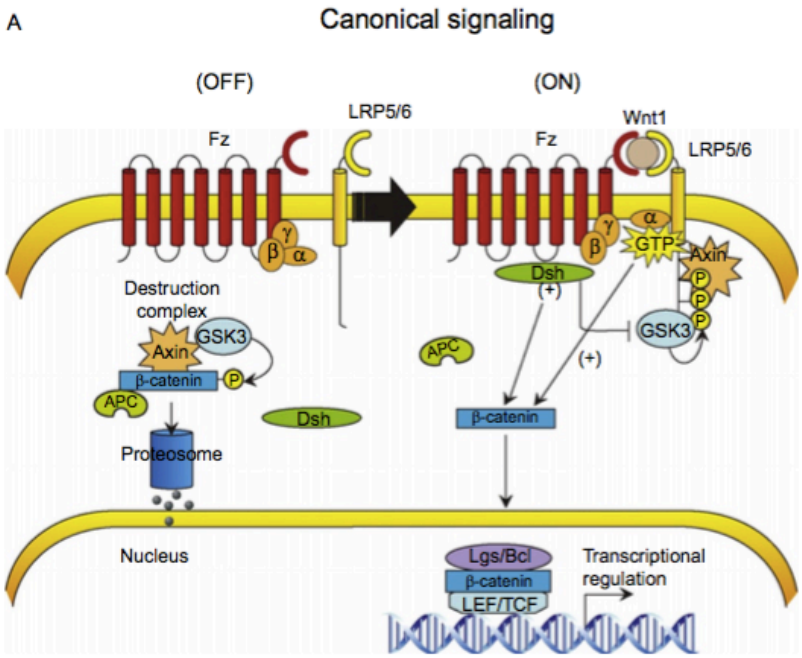

Figure 6 - ***Canonical Wnt Signaling.***
On the "OFF" side of the diagram it is possible to observe β-Catenin being degraded by the Axin Complex and the proteasome. On the "On" side of the diagram Wnt binds to frizzle and LRP5/6, recruiting the Axin Complex and stopping β-Catenin degradation (Adapted from Flaherty, Kamerzell, & Dawn, 2012).

2.6. Absence of Cerl2 leads to Heart defects

The heart presents cellular and molecular left-right differences, suggesting that the heart is lateralized from its inception and throughout its development. The first evidence of asymmetry in the heart development is when it undergoes looping morphogenesis and then all its development, including chamber formation, inflow and outflow track formation and the position of the heart relative to the midline also exhibit L-R differences (Ramsdell, 2005). As explained previously, the

symmetry of the embryo is broken, at the node, by a cascade of gene activation that will express different properties on the left and right sides of the embryo. Any impairment on the L-R axis formation can lead to laterality defects and is, usually, also responsible for particular types of congenital heart defects (Icardo et al., 2002) (Ramsdell, 2005). These congenital heart defects are commonly related to L-R defects during cardiac development and include transposition of the great arteries, double outlet right ventricle, pulmonary stenosis or atresia, anomalous pulmonary venous return, systemic venous anomalies, ventricular and atrial septal defects, single ventricle, and rhythm disorders (Desgrange, Le Garrec & Meilhac, 2018). However, in 2014, Araújo and her colleagues reported that defects in *Cerl2* (a crucial gene for the L-R axis establishment) leads to cardiac defects that cannot be explained by laterality abnormalities. They have analyzed a *Cerl2* knockout mouse line and stated a significantly high mortality rate of neonates, mostly due to cardiac defects. These mice presented a large increase in the left ventricular myocardial wall and systolic dysfunction incompatible with a long lifespan. Further studies to these hearts showed that the increased ventricular muscle was due to a high proliferation of cardiomyocytes. Expression levels of Cerl2 on the left ventricle were significantly higher than on the right ventricle, leading the authors to hypothesize the importance of this gene for the ventricular myocardial formation. Moreover, the levels of phosphorylated Smad2 (ρ-Smad2) were also increased on the left ventricle of both embryonic and neonatal hearts, indicating that the TGF-β/Nodal signaling was activated for a long period of time. Therefore, validating the role of Cerl2 in exerting a negative feedback for the TGF-β/Nodal signaling in the heart development, independent of its major role in the left-right axis establishment (Araújo, Marques & Belo, 2014). Unpublished data from the lab has also reported an increase of Wnt signaling in the *Cerl2* knockout mice hearts, leading to the hypothesis of this single gene as a potencial regulator of both Nodal and Wnt pathways, in the heart formation, and possibly modulating the cardiomyocyte yield, thus explaining the phenotype observed in the *Cerl2* knockout mice.

2.7. Mouse Embryonic Stem Cells

Embryonic stem cells (ESCs) can be derived from the inner cell mass (ICM) of a mouse embryo at blastocyst stage. These types of cells have an unlimited ability to proliferate indefinitely (or self-renew) in vitro while maintaining pluripotency. Moreover, they present the capacity to differentiate into all the cell types derived from the three primordial germ layers, offering a very promising potential as a source of cells for heart regeneration.

2.7.1. *In Vitro* Culture

Back in 1981, Evans & Kaufman successfully derived for the first-time mouse pluripotent cells *in vitro* from preimplantation mouse embryos (Evans & Kaufman, 1981) (Martin, 1981). They named those cells as "embryonic stem cells" and established the elementary principles to derive mouse ES cells, consisting in co-culture blastocysts with a feeder layer of mitotically arrested mouse embryonic fibroblasts (MEF) and medium containing carefully screened fetal calf serum (FCS) (Evans & Kaufman, 1981) (Martin, 1981) (Robertson, 1987). Using these culture conditions, the investigators expected to promote the proliferation of ESCs colonies while maintaining a pluripotent and undifferentiated phenotype. Subsequent work aimed on characterizing the molecular pathways supporting the maintenance of pluripotency in ESCs. In 1988, researchers identified cytokine leukemia inhibitory factor (LIF) as the principal component produced by feeder cells (M. Williams et al., 2011) (Smith et al., 1988). LIF can also support ES cell maintenance without feeders in either serum or bone morphogenetic protein (BMP) (Nichols et al., 1990; Ying et al.,2003a). In these conditions, however, the cultures are morphologically heterogeneous because feeder cells provide an additional attachment matrix as well as factors in addition to LIF (M. Williams et al., 2011) (Smith et al., 1988). LIF is an important cytokine belonging to the interleukin 6 (*Il-6*) family that activates STAT3 which feeds the pluripotency network by upregulating the expression of pluripotency factors such as *KLF4*, *Gbx2*, and *Tfcp2l1* (Niwa et al., 2009) (Tai & Ying, 2013). Factors presenting in the serum, principally bone morphogenetic proteins, stimulate the SMAD signaling pathway and constrain lineage commitment by inducing expression of inhibitor of differentiation proteins (Ying et al., 2003) (Malaguti et al., 2013). Taking this into account, Ying et al., in 2008, reported a new stem cell culture system to maintain ESCs in the absence of LIF, serum, and feeders, using two small molecule inhibitors termed "2i." The culture components of "2i medium" are two chemical kinase inhibitors, PD03 (PD0325901) and CHIRON (CHIR99021) which modulate key pathways involved in lineage commitment and pluripotency (Ying et al., 2008). PD03 is a MEK inhibitor which blocks the auto-inductive effects of the FGF/ERK1/2 signaling cascade on differentiation, while CHIRON inhibits GSK-3 which mimics the effects of canonical Wnt signaling and thereby alleviates the repressive effects of TCF3 on pluripotency genes (Ying et al., 2008). Importantly, under 2i condition medium, it was possible to derive ES cells from strains previously impossible, including the NOD strain (Hanna et al., 2009) (Ying et al., 2008), and was possible to retain a euploid karyotype and germline chimaera competency of male ES cells over multiple passages with similar efficiency to cells cultured in

serum (Ying et al., 2008). Therefore, the use of culture medium supplemented with LIF and the 2i conditions, allows the maintenance of stemness in culture, for prolonged time, with the cells retaining their self-renewing capacity and reducing significantly spontaneous differentiation events along time, providing a so-called ground state of pluripotency.

2.7.2. Modulation of Cardiac Differentiation

Embryonic stem cells have emerged as a promising source of cells to solve the unmet medical problem of restoring heart function through heart regeneration. In fact, in nowadays, it is possible to manipulate and differentiate ESCs towards a cardiac lineage, recapitulating the crucial steps for proper cardiac specification. Investigators are now capable to derive cardiomyocytes that can be specified into nodal, working, and conduction system myocardium. However, the specification of the cardiovascular lineages involves a transition through a sequence of increasingly restricted progenitor cells, starting from a pluripotent state to mesoderm and then commitment and specification of cells to cardiovascular fates (Figure 7).

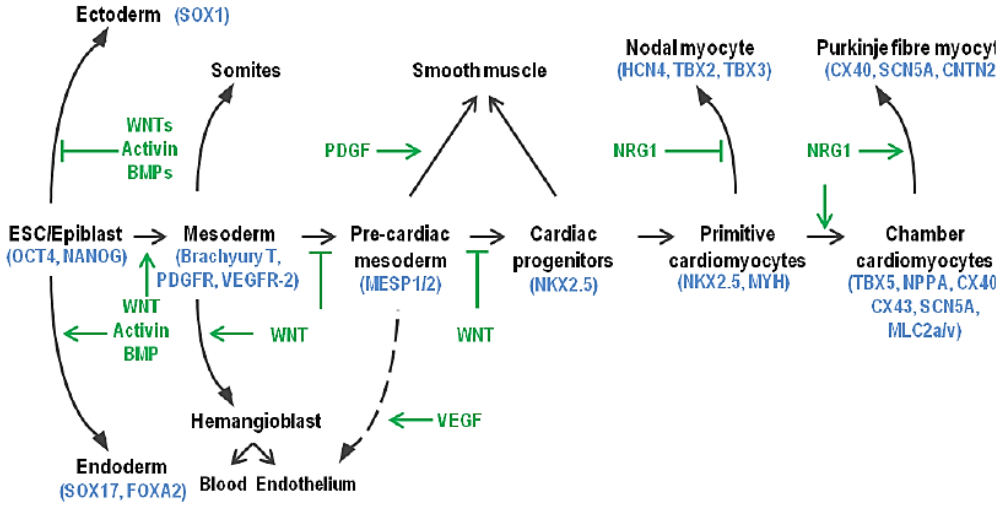

Figure 7 - ***Growth factors and key transcription factors that regulate fate choices during early embryonic cardiogenesis and ESCs differentiation.***
Growth factors that regulate fate choices are listed at branch points (green), and key transcription factors and surface markers for each cell state are listed under the cell types (blue). BMPs, bone morphogenetic proteins; CNTN2, contactin-2; CX, connexin; FOXA2, forkhead box protein A2; HCN4, potassium/sodium hyperpolarization-activated cyclic nucleotide-gated channel 4; MESP, mesoderm posterior protein; MLC2a/v, myosin light chain 2a and/or 2v; MYH, myosin heavy chain; NPPA, natriuretic peptide precursor A; NRG1, neuregulin 1; PDGF, platelet-derived growth factor; PDGFR, PDGF receptor; SCN5A, sodium channel protein type 5 subunit α; SOX, SRY-related high-mobility-group box; TBX, T-box transcription factor; VEGF, vascular endothelial growth factor; VEGFR-2, VEGF receptor-2 (adapted from Laflamme & Murry, 2011)

Culturing and differentiating mouse stem cells as aggregates structures, called embryoid bodies (EBs), has become a routine protocol in many laboratories since in 1985, when Doetschman and colleagues shown that the spontaneous in vitro differentiation of ESCs could give rise to cells from the 3 embryonic germ-layers (Doetschman et al., 1985). Taking advantage of this capacity,

researchers have been using EBs to understand the early events of mammalian embryogenesis and study differentiated cells derived from the germ layers, including cardiomyocytes (Desbaillets et al., 2000). The protocol of spontaneous differentiation is triggered after the removal of LIF from the culture medium and cultivating the cells using the hanging drop culture technique (Figure 8).

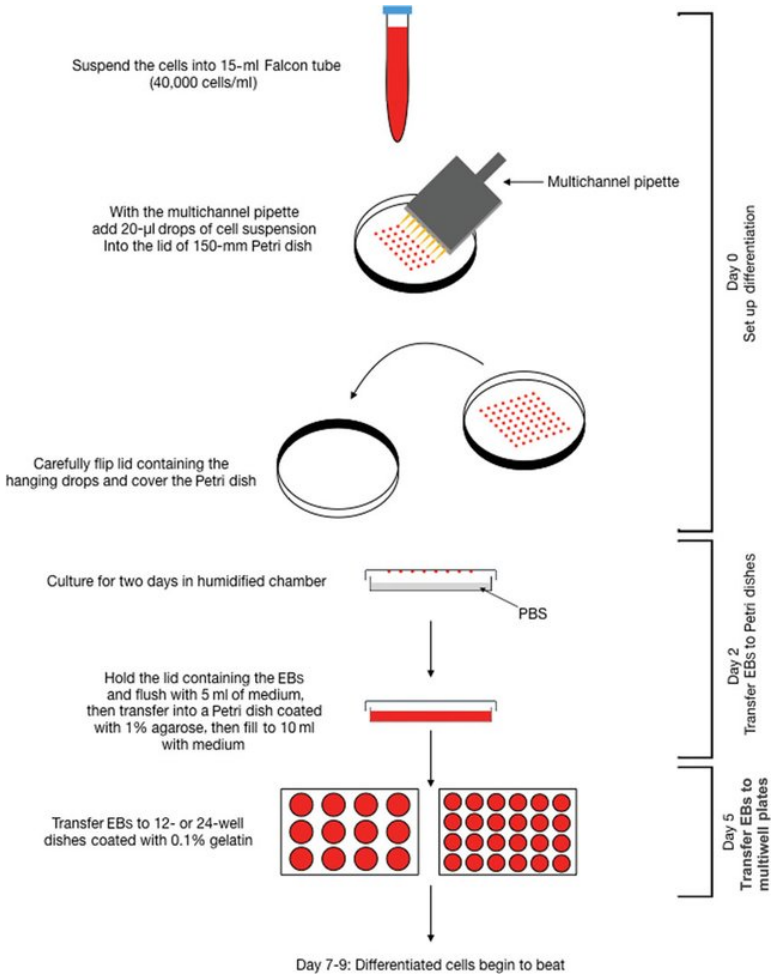

Figure 8 - ***Schematic representation of the hanging droplet method used to differentiate ESCs.***

Undifferentiated ESCs are maintained in culture for 2 passages prior to differentiation with medium supplemented with LIF. A cell suspension is prepared and cells are put to grow in droplets on an inverted bacterial dish for 2 days, and EBs grow in suspension three additional days. At day 5 of differentiation the formed EBs are plated in to gelatin-coated 6-well plates (adapted from Combinatorial Utilization of Murine Embryonic Stem Cells andIn Vivo Modelsto Study Human Congenital Heart Disease)

This technique, which requires the cultured of the cells with a precise density (normally 500 cells per drop) in hanging drops and in inverted bacterial-grade dishes, allows the aggregation ES cells to encounter each other, as a stochastic event, forming the 3-dimentional EBs with the stimulus of the gravity and by no adherence to the culture dishes (Kurosawa, 2007) (Weitzer, 2006). After 24 hours in culture, EBs aggregations resemble the inner cell mass of embryos, with irregular surfaces (Weitzer, 2006). From day 1 to day 3 EBs continue to increase in size forming an outer shell-like layer composed of cells and an enriched collagen IV and laminin extracellular matrix (ECM), that

can act similar to the endoderm in the embryos by secreting mesoderm inducing morphogens (Li et al., 2001). Moreover, during this time, cells lose the expression of pluripotency markers Oct4, Nanog and Sox2 and start to express germ-layer specific genes like α-Fetoprotein (AFP) and Brachyury (T), which is responsible for inducing mesoderm formation (Weitzer, 2006). Around day 4, cells start to have a transient expression of *Mesp1*, marking the first sign of early cardiac commitment. Similarly, in the embryo, Mesp1 expression can be found transiently at E6.5 stage in the cells of the primitive streak that will migrate to the cranial region to form the cardiac progenitors that will populate the first and second heart fields (Weitzer 2006) (Saga et al., 1996). After day 4, different early cardiac markers start to be expressed in the EBs, such as *Nkx2.5* and *Isl1*. *Nkx2.5* and *Isl1* are critical transcription markers of FHF and SHF cells' lineage, respectively (Meilhac et al., 2014). After plating the EBs on gelatin-coated culture dishes at day 5, they start to form cellular structures that within a couple of days start beating and are called beating foci. These structures represent the first sign of mature cardiac differentiation, and are marked for the expression of cardiac *Troponin T* (TnT) and myosin chains encoding genes (light and heavy chains) (Weitzer 2006). Until the end of the differentiation protocol at day 10, the beating foci maturate, showing identical action potentials' shape compared to those measured in primary cultures of embryonic cardiomyocytes (Maltsev et al., 1993)

Although this method to differentiate stem cells towards a cardiomyocyte lineage correlates appropriately with the developmental stages and to what occurs in vivo mouse embryos, this suspension culture technique has some inherent limitations and disadvantages. For instance, one of the biggest limitations of this technique is the lower percentage of cardiomyocytes' production. To overcome this, we proposed to develop an optimized spontaneous differentiation protocol by modulating two critical pathways, Nodal and Wnt signaling pathways, acting during cardiac specification and involved in the two mechanisms that generate CMs: differentiation of CPCs; and proliferation of mature CMs.

3. MATERIALS AND METHODS

3.1. Cell Culture

Handling of the cells, medium preparation and other techniques that require aseptic conditions were performed in laminar flow cabinet after irradiation for 15 minutes with ultraviolet (UV) light. Cells were cultured in a humidified incubator at 37ºC with 5% of CO_2 and microscopic examination of cell growth was performed frequently by using an inverted light microscope, Evos XL Core (Thermo Scientific)

3.2. Culture of primary mouse ESC

Established Wild-type (WT) and Knockout (KO) *Cerl2*$^{-/-}$ primary cell lines used in this work were derived from blastocysts of corresponding WT and Cerl2 KO mice, according to a previous work, developed in our lab (unpublished data). Cells were cultured in 0.1% gelatin coated wells (6-well plate), with ES cell medium composed of Knockout-DMEM medium (Gibco® Life Technologies) supplemented with 15% FBS (HyClone, Thermo Scientific), 1% MEM Non-Essential Amino Acids (Gibco® Life Technologies), 1% Penicillin/Streptomycin, 2 mM L-glutamine and 0.1 mM β-Mercaptoethanol (Gibco® Life Technologies). To maintain pluripotency conditions of the ESCs, 5 x 10^5 U mouse leukaemia inhibitory factor (LIF; ESGRO® Millipore),50 mM PD0325901 (Calbiochem® Millipore) and 10 mM CHIRON99021 (Calbiochem® Millipore) inhibitors were added to the ES cell medium. Medium was changed every day.

As soon as ESCs reach 70% confluency they were passaged to a new well in a 6-well plate. To pass the cells, the medium was removed, the cells washed with PBS 1x and then trypsinized with 0.5mL of Trypsin 1x followed by 5 min incubation at 37° C. Subsequently, the trypsin was inactivated by adding 3mL of ES cell medium and the cell suspension was pipetted up and down, gently, to ensure a single-cell suspension to be centrifuged at 1000rpm for 3min. The supernatant was discarded and fresh ES cell medium was added to resuspend the pellet. Finnaly the cells were plated with a 1:10 dilution factor in a 6-well plate and incubated at 37ºC with 5% CO_2.

3.3. Cardiac spontaneous differentiation of ESCs

Cardiac spontaneous differentiation of wild type (WT) and knockout *Cerl2*$^{-/-}$ mouse ESCs lines were accomplished using the hanging droplet method to generate embryoid bodies (EBs; figure 1) previously described in the literature (Keller, 2005).

Briefly, undifferentiated ES cells were washed with PBS 1x, incubated with 0.5mL of Trypsin 1x at 37° C, for 5 minutes, dissociated to form a single cell suspension, centrifuged and resuspended in

fresh ESC medium without LIF and the inhibitors. Cells were counted using a Nebauer chamber in order to prepare a cell suspension with a final concentration of $2.5x10^4$ cells/mL. Cells were then plated as 20µL drops (~500 cells) onto an anti-adherent Petri dish using a multichamber pipette. The Petri dish was then inverted and 3mL of PBS were added to the lid to create a humidified atmosphere. The cells were allowed to grow in hanging drop suspension for two days (days 1 and 2 of differentiation), at 37º C and 5% CO_2, to form the EBs aggregations. At day 2 of differentiation the Petri dishes were inverted to its original position and 8mL of ES cell medium, without LIF and inhibitors, was added to the plates. EBs were cultured in suspension until day 5 of differentiation, when they were plated in 0.1% gelatin coated wells and cultured until day 10 of differentiation, to promote spontaneous differentiation. During all the period of cardiac differentiation, the morphology and the growth of the EBs were closely monitored and cell samples were collected for each differentiation day.

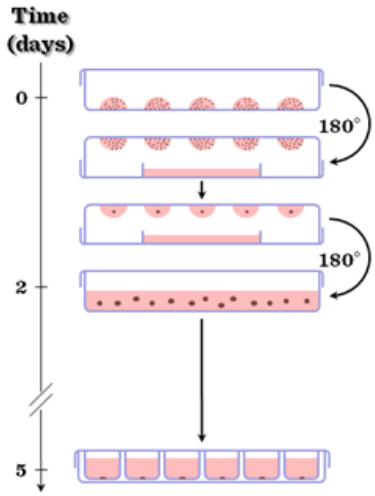

Figure 9 - ***Schematic of the embryoid bodies protocol for cardiomyocytes spontaneous differentiation, for Western Blot and qPCR analysis.*** (Adapted from Digitális Tankönyvtár, 2018).

3.3.1. TGF-β/Nodal and Wnt/β-Catenin signaling induction

To test the effect, separately or together, of increased levels of TGF-β/Nodal and Wnt//β-Catenin signaling pathways during the process of cardiac differentiation in the WT cell line, these pathways were induced separately and simultaneously at day 2 of the cardiac spontaneous differentiation protocol. To induce TGF-β/Nodal signaling, 4ng/mL of Activin A prepared in 0,1% of BSA in PBS was added to the ES cell medium at day 2 of differentiation. For the activation of Wnt/β-Catenin signaling, 10µM (this concentration was later adjusted to 5µM) of CHIR99021 (Stemgent®) dissolved in DMSO was added to ES cell medium at day 2 of differentiation. As control, an equal volume of 0.1% BSA in PBS or DMSO, without the activator molecules, was added to the ES cell

medium of the WT stem cell line. In some conditions, at day 3 of differentiation, half of the medium (4mL) was replaced by new medium with CHIR and/or Activin A, using the same concentrations as described previously. For the rest of the conditions, at day 3 of differentiation, the medium was totally replaced by new ES cell medium, without the molecules, to stop the induction of the pathways.

3.4. Protein Extraction and Quantification

Total protein was extracted using a Tropix Buffer solution, pH 7.8, containing Triton X-100 0,2% V/V and Monopotassium phosphate (KH_2PO_4) 10nM, Ditiotreitol (DTT) and a cocktail of protease and phosphatase inhibitor. Samples were quantified using the Bradford (Sigma®) method as described by the manufacture: Bovine serum albumin (BSA) was used to obtain a calibration curve and samples were read at 595nm.

3.5. Western-Blot

Total protein extracts were heated at 100ºC for 5 min for denaturation and proteins were separated by their molecular weight in an 8% or 12% SDS-PAGE polyacrylamide gel through electrophoresis. The proteins on the gel were then transferred to a nitrocellulose membrane or polyvinylidene difluoride (PVDF) membrane activated with methanol and blocked with 5% BSA to prevent both unwanted membrane-protein interaction and interaction with an antibody for a phosphorylated protein that was used. Subsequently, the membranes were incubated overnight, at 4°C, with the respective primary antibody. On the next day, to identify the primary antibody protein complexes, the membranes were incubated with a secondary antibody for one hour, at room temperature. The secondary antibody is conjugated with the Horseradish Peroxidase (HRP) enzyme to produce a signal for detection on Chemidoc, by densitometry. The intensity of the bands was quantified and the values were normalized with tubulin, used as loading control.

Table 1 - ***Proteins and Antibodies information for Western Blot.***

Protein	Primary Antibody (IAb)	IAb Concentration	Secundary Antibody (IIAb)	IIAb Concentration	Molecular Weight (kDa)
β-Catenin	Anti-β-Catenin Santa Cruz Biotechnology® sc-7963	1:1000	Anti-Mouse Sigma® A4416	1:2000	92
ρ-Smad2/3	Anti-ρ-Smad2/3 Cell Signaling® #3101	1:500	Anti-Rabbit Vector Laboratories® BA-4001	1:5000	60
Smad 2/3	Anti-Smad2/3 Cell Signaling® #3102	1:500	Anti-Rabbit Vector Laboratories® BA-4001	1:5000	60
Tubulin	Anti-Tubulin Sigma® T6199	1:10000	Anti-Mouse Sigma® A4416	1:2000	50

3.6. Immunofluorescence

WT and KO mouse embryonic stem cells were plated over a coverslip coated with 0,1% gelatin and were allowed to grow for 2 days. Afterwards, cells were rinsed with room-temperature PBS 1X and fixed with 4% paraformaldehyde (PFA), 15 min at room temperature, next, cells were washed three times with PBS 1X, 10min each and then, permeabilized using 0.1% PBS Triton X-100, 30 min at room temperature. Unspecific antibody-binding sites the cells were blocked with a solution composed of 1X PBS, glycine, 1% BSA and 0,05% sodium azide, overnight at 4°C, to block. The cells were then incubated at 4° C overnight with primary antibodies against markers of pluripotency (*Nanog*, *Oct4* and *SSEA1*), as shown in table 2. After four washes of 10min each, with blocking solution, secondary antibodies, Donkey Anti-Rabbit and Donkey Anti-Mouse, were placed on the cells and incubated for 2h at room temperature. The presence and distribution of Nanog, Oct4 and SSEA1 in the WT and KO were acquired with Zeiss Axio Imager Z2 microscope (Carl Zeiss). Images were posteriorly adjusted using ImageJ software.

*Table 2 - **Antibodies used for Immunofluorescence**.*

Protein	Primary Antibody (IAb)	IAb Concentration	Secundary Antibody (IIAb)	IIAb Concentration
Nanog	Anti-Nanog	1:150	Donkey anti-rabbit Invitrogen® Alexa Fluor 488	1:500
Oct4	Anti-Oct4	1:150	Donkey anti-rabbit Invitrogen® Alexa Fluor 488	1:500
SSEA1	Anti-SSEA1	1:50	Donkey anti-mouse Invitrogen® Alexa Fluor 488	1:500

3.7. RNA Extraction and cDNA synthesis

Total RNA was extracted and purified from mouse WT and KO stem cells lines for all the several tested conditions, for each differentiation day, using 300µL of TRI Reagent® (Sigma), plus do Direct-zol™ RNA MiniPrep Kit (Zymo Research). After lysing the cells with TRI Reagent®, samples were frozen at -80°C until the extraction and purification were performed. For the extraction, samples were thawed and added an equal volume of 99% ethanol and mixed thoroughly, to precipitate DNA and RNA. Next, the samples were treated with Direct-zol™ RNA MiniPrep Kit (Zymo Research) according to the manufacturer's instructions. Purified RNA samples were eluted in 30µL of nuclease-free water, provided in the kit. Finally, samples were analyzed for their quantity and quality, using a spectrophotometer (Nanodrop 2000, Thermo Scientific). The purified RNA was kept at -80°C, until further analysis.

Complementary DNA (cDNA) was generated from an RNA template by a reverse transcription reaction, composed of two steps. First, 1µg of RNA, 0.5µg of Oligo (dT) primers and RNase-free water up to 11.5µL was prepared and incubated, 5min at 65°C, in order to promote the annealing of the oligo (dT) primers with the single-stranded RNA template. Later, a master mix solution containing 4 µL of 5x Reaction Buffer, 40 U/µL of RiboLock RNase Inhibitor, 200 U/µL of RevertAid Reverse Transcriptase and 10 mM of dNTP, making a total 20µL volume per sample was added to the previous reaction. Subsequently, samples were incubated at 42°C for 1 hour, followed by the step of denaturation at 70°C for 10 minutes. DNA strands were polymerized followed by the deactivation of the reverse transcriptase enzyme. Finally, cDNA samples were diluted in a 1:10 ratio with nuclease-free water and stored at -20°C.

3.8. qRT-PCR

Triplicate reactions were performed in 96-well plates using optical sealing tape for a 15µL total volume for each. Each qRT-PCR reaction contained 7.5 µL of power SYBR® Green Master Mix (Applied Biosystems), 2 µL of cDNA, 0.1 µM of each forward and reverse primers and ultrapure water up to the final desired volume. The amplification and fluorescent detection were performed with Thermo QuantStudio 5 Real-Time PCR machine. The program for amplification of target sequences was as follow: initial step of denaturation at 95°C for 2 minutes, followed by 40 cycles of denaturation step at 95°C for 10 seconds, annealing for 10 seconds at the gene-specific annealing temperature (Table 3) and an extension step at 72°C for 20 seconds. Relative quantification of expression was performed using the ddCt method (Bustin, 2000) and normalized to GAPDH and PGK1 as housekeeping genes. Day 0 of differentiation was used as reference. The oligonucleotide primer sequences used and respective annealing temperatures are listed in table 3.

*Table 3 - **qRT-PCR primers used in this work and respective annealing temperatures**.*

Gene	Forward Primer	Reverse Primer	Annealing Temperature (°C)
GAPDH	5' GGGAAGCCCATCACCATCTTC 3'	5' AGAGGGGCCATCCAAGTCT 3'	61
PGK1	5' ATGGATGAGGTGGTGAAAGC 3'	5' CAGTGCTCACATGGCTGACT 3'	58
Nodal	5' CCAGACAGAAGCCAACT 3'	5' AAGCATGCTCAGTGGCT 3'	60
Pitx2	5' AAGCCACTTTCCAGAGAAACC 3'	5' AAGCCATTCTTGCACAGCTC 3'	58
β-Catenin	5' ATGGAGCCGGACAGAAAAGC 3'	5' CTTGCCACTCAGGGAAGGA 3'	55
Wnt3a	5' TCACTGCGAAAGCTACTCCA 3'	5' CACCACCGTCAGCAACAG 3'	59
Nkx2.5	5' CCACTCTCTGCTACCCACCT 3'	5' CCAGGTTCAGGATGTCTTTGA 3'	60
Isl1	5' CCTGTGTGTTGGTTGCGGCA 3'	5' GGGCACGCATCACGAAGTCG 3'	62
Cerl2	5' GCAGAGAGTAGCTGCTGGTGTGCCTTT 3'	5' CGGCACACAGCTGTTGCAGAAGACTAC 3'	68
α-MHC	5' GATGGCACAGAAGATGCTGA 3'	5' CTGCCCCTTGGTGACATACT 3'	60

3.9. Statistical Analysis

Statistical Analysis was performed using *GraphPad Prism 6* software for Windows (GraphPad Software, Inc; San Diego California, USA). All the experimental values are reported as mean ± SD. For the RT-PCR experiments, the statistical differences between the two groups WT/KO and No Induction/With Induction were determined by applying the Two-way ANOVA Multiple

Comparisons Bonferroni test. To reject the null hypothesis, the probability values of *P<0.05 were considered statistically significant.

4. RESULTS AND DISCUSSION

4.1. Pluripotency properties of WT and Cerl2 KO cell lines

The importance of Cerl2 in the L-R axis formation has already been established and any impairment in this gene can lead to L-R abnormalities, known as heterotaxia, as well as, congenital heart defects (Belo et al., 2017). Recently this gene has been implied in some congenital heart defects that cannot be explained by laterality defects. The analysis of *Cerl2* knockout mice present a high mortality rate at birth due to hyperplasia of the left ventricle and systolic dysfunction incompatible with a long lifespan (Araújo, Marques & Belo, 2014). In order to study these cardiac abnormalities, a previous thesis work of the lab, has generated a *Cerl2* KO mouse embryonic stem cell lines from *Cerl2* KO mice as a tool to investigate the molecular and genetic mechanisms that lead to disease. In the present work, this cell line was differentiated into cardiomyocytes, and its potential as disease model explored.

Firstly, its pluripotency was re-accessed by immunofluorescence for markers of pluripotency. For this assessment, it was used two nuclear markers – NANOG and OCT4 – and one surface marker – SSEA1. For a cellular quantification control, the cells were stained with DAPI that exclusively marks the A-T rich regions of the DNA in the nucleus. The colonies from both cell lines presented positive signal for all the pluripotency markers (Figure 8A representing the WT cells and Figure 8B the KO ones). On the edges of the colonies, in the merged images, it is noticed that some cells show reduced positive signal for NANOG and OCT4, this can be explained by a diminution of pluripotency on the borders of the colonies, indicating some spontaneous differentiation.

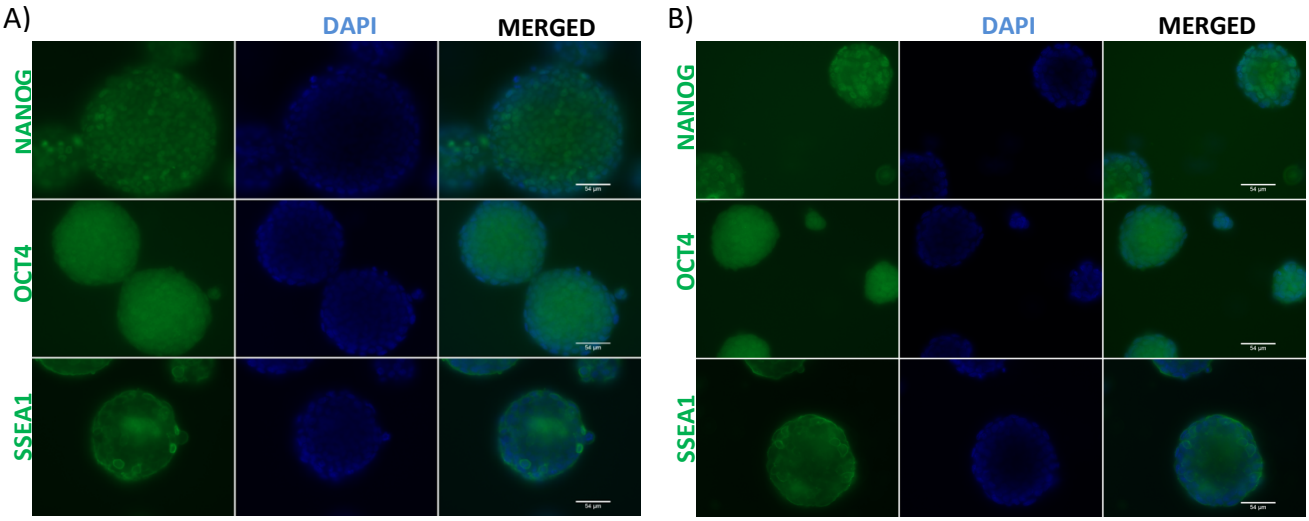

Figure 10 - ***Expression of NANOG, OCT4 and SSEA1 in WT and Cerl2$^{-/-}$ ES cells.***

Immunofluorescence analysis show positive protein expression for the referred regulator markers of pluripotency in mouse *Cerl2*$^{-/-}$ ES cells derived from: (A) WT cells and (B) KO cells. Scale bars: 54µm.

4.2. Differentiation into Cardiomyocytes of WT and Cerl2 KO cells

After positively assessing the pluripotency properties of the WT and *Cerl2* KO cells lines, they could be used as a reliable *in vitro* model to study cardiac differentiation from mESCs, focusing on the Nodal and Wnt pathways. After each passage the cells were maintained in ESC medium with the MEK and GSK3 inhibitors (2i), in order to sustain the pluripotency of the cells. MEK inhibitor blocks the auto-inductive effects of the FGF/ERK1/2 signaling cascade on differentiation, while the GSK-3 inhibitor stops the β-Catenin degradation, which will mimic the effects of canonical Wnt signaling and thereby alleviates the repressive effects of TCF3 on pluripotency genes (Ying et al., 2008). However, on the previous day of the cardiac differentiation protocol begins, the cell medium was changed to ESC medium without the 2i, only with LIF to prevent spontaneous differentiation. This was performed to prevent the extension of Wnt signaling and other signaling pathways involved in the pluripotency stage, during the differentiation protocol. Since this pluripotency stage happens transiently *in vivo*, it was recently demonstrated that prolonged culture of ES cells with 2i results in irreversible epigenetic and genomic changes that will impair their development ability (Choi et al., 2017), so the use of these two molecules was performed for brief periods of time (ex: cell passage).

The cardiac differentiation for the pluripotent WT and *Cerl2* KO cells was performed in parallel, by the hanging drop method (Figure8), leading to the Embryoid Bodies formation. At day 0 of differentiation the ES cells were detached from the gelatin coated wells and resuspend in ES medium without LIF, to be prepared in a specific and comparable concentration (500 cells per drop) in each Petri dish for the *Cerl2* KO and for the WT ES cell lines. The cells are incubated in a hanging drop manner for 48H, during this period the gravity effect will induce stochastic events on the cells, inducing their aggregation into 3D structures (Kurosawa, 2007). Then, at day 2 of differentiation, the plates were inverted and the formed EBs were maintained in suspension culture until day 5 of differentiation, allowing their growth and consequent stimulation of the specific germ layer differentiation. Subsequently, at day 5 of differentiation the EBs were plated in gelatin coated 6-wells plates, the same number of EBs was plated in each well to perform a normalized comparison of the cardiac differentiation capacity between WT and *Cerl2* KO cell lines. The plated EBs were carefully selected, in order to avoid abnormally shaped or aggregated EBs, as anomalous EBs will not proliferate and differentiate as expected, also presenting an increase in the cell death's phenomena. These slight changes can affect the neighbor EBs and impair their efficiency of cardiomyogenesis (Rungarunlert, 2009). The spontaneous differentiation was

maintained until day 8 and the EBs were monitored every day (Figure 9). The KO EBs usually started showing contractile movements at day 6, one day before the WT EBs, that usually started showing contractile movements at day 6/7 of differentiation. Furthermore, as observed in the previous work performed in the lab, the *Cerl2* KO EBs showed more beating foci than the WT ones, withstanding the hyperplasia phenotype observed *in vivo.*

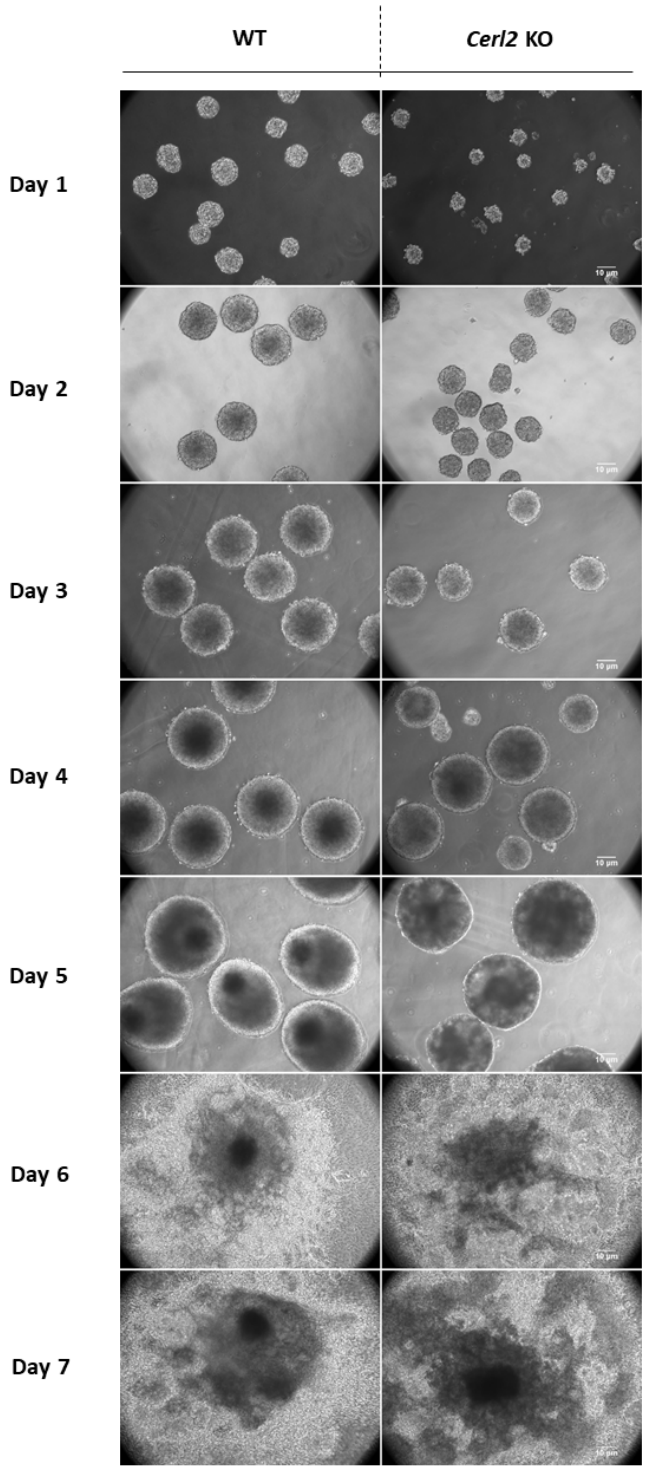

Figure 11 – ***Overview of the Morphology of the derived WT and KO EBs at several differentiation days of the protocol***. Until day 5 all the EBs showed a round shape, with irregular surface protrusions, specially the KO ones. After day 5 the EBs were plated and started expanding. Scale bars: 10µm.

With the purpose of studying the expression levels of signaling pathways and cardiac markers, RNA and protein samples were collected at each day of differentiation. The RNA samples were used to synthesize cDNA, which was utilized as a template for RT-PCR experiments. It is known that *Cerl2* starts to be expressed asymmetrically on the right side of the mouse node, suppressing the expression of the Nodal signaling pathway on this side. This asymmetric expression of Nodal is latter on translocated to the LPM (Oki et al., 2007). This occurs during the first stages of cardiac differentiation so it is expected a *Cerl2* expression peak during these early stages on the WT EBs. Indeed, the expression of *Cerl2* peaked at day 4 of differentiation as observed by RT-PCR (Figure 10), then the expression values decreased and a second upregulation is visible at day 8. At this timepoint (day8), the cardiomyocytes start to differentiate into specific cardiac lineages (Weitzer 2006), so it is possible that Cerl2 is being recruited to regulated the pathways involved in proliferation and specification of cardiomyocytes.

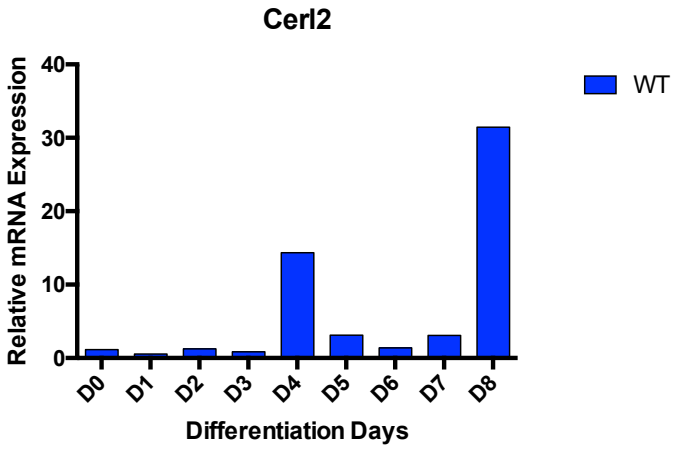

Figure 12 - ***Relative mRNA expression of Cerl2 in the WT differentiated cells.***
qRT-PCR experiments performed for WT differentiated cells of one differentiation, for Cerl2. No statistical test was applied.

Studies reported an increase in the ventricle myocardial wall due to cardiomyocyte hyperplasia in the *Cerl2* KO mice (Araújo, et al., 2014) and previous unpublished work performed in the lab showed that the expression of both early and late cardiac markers was upregulated on the *Cerl2* KO differentiated cells. The FHF progenitors can be identified by the positive expression marker of the Nkx2.5 gene (Bruneau, 2002). This structure will contribute to the formation of the linear tube and later give rise to the mature cardiac cells of the left ventricle (Bruneau, 2002). Corroborating the previous work performed in the lab, the KO differentiated cells presented higher expression levels of the NKx2.5 marker, than the WT differentiated cells (Figure 11). Although the differences were not statistically significant, possibly due to the high standard deviation levels, it is possible to perceive a clear tendency. This upregulation further validates the hypothesis that a higher number of FHF progenitors during mouse cardiogenesis, of the *Cerl2* KO mice, leads to a robust

myocardium tissue, comparatively to the control levels. In addition to the Nkx2.5 marker, the Isl1 marker was also assessed (Figure 13A and B). This gene is expressed on the SHF cells, being these cells the late cardiac progenitors for myocardial, endothelial and smooth muscle cells (Bruneau, 2002). The *Isl1* levels did not present statistically significant differences but the same tendency of the Nkx2.5 marker is visible. On the KO differentiated cells there is an upregulation of the Isl1, from day 4, reaching its peak at day 7, whereas, in the WT differentiated cells the peak it's a day 7 but with lower expression levels (Figure 13B). These results point to a higher expression of cardiac progenitors but it was also important to evaluate the functionality state of cardiomyocyte's maturation. Myosin is an important protein for the generation of contractile movements in the heart muscle. Two Myosin Heavy Chain genes are expressed in the mammalian heart - α-MHC and β-MHC - the α-Myosin Heavy Chain (α-MHC) is a cardiac-muscle specific protein involved in active force generation (Molkentin, 1996). Considering the RT-PCR expression levels of α-MHC (Figure 13C), there was a visible alteration at day 6 with the *Cerl2* KO differentiated cells presenting higher levels of this markers and this tendency is also visible at day 8. This difference may indicate the presence of more cardiomyocytes in the *Cerl2* KO differentiated cells, as possible consequence of the intensified stimulation of KO cardiomyogenesis resulted from the loss-of-function of *Cerl2*. The graphs present high standard deviations, this happens because only two differentiations are being analyzed, in order to decrease the standard deviations, more experiments should be performed and analyzed. Moreover, the experimental conditions of the differentiations should be improved to avoid differences between each differentiation.

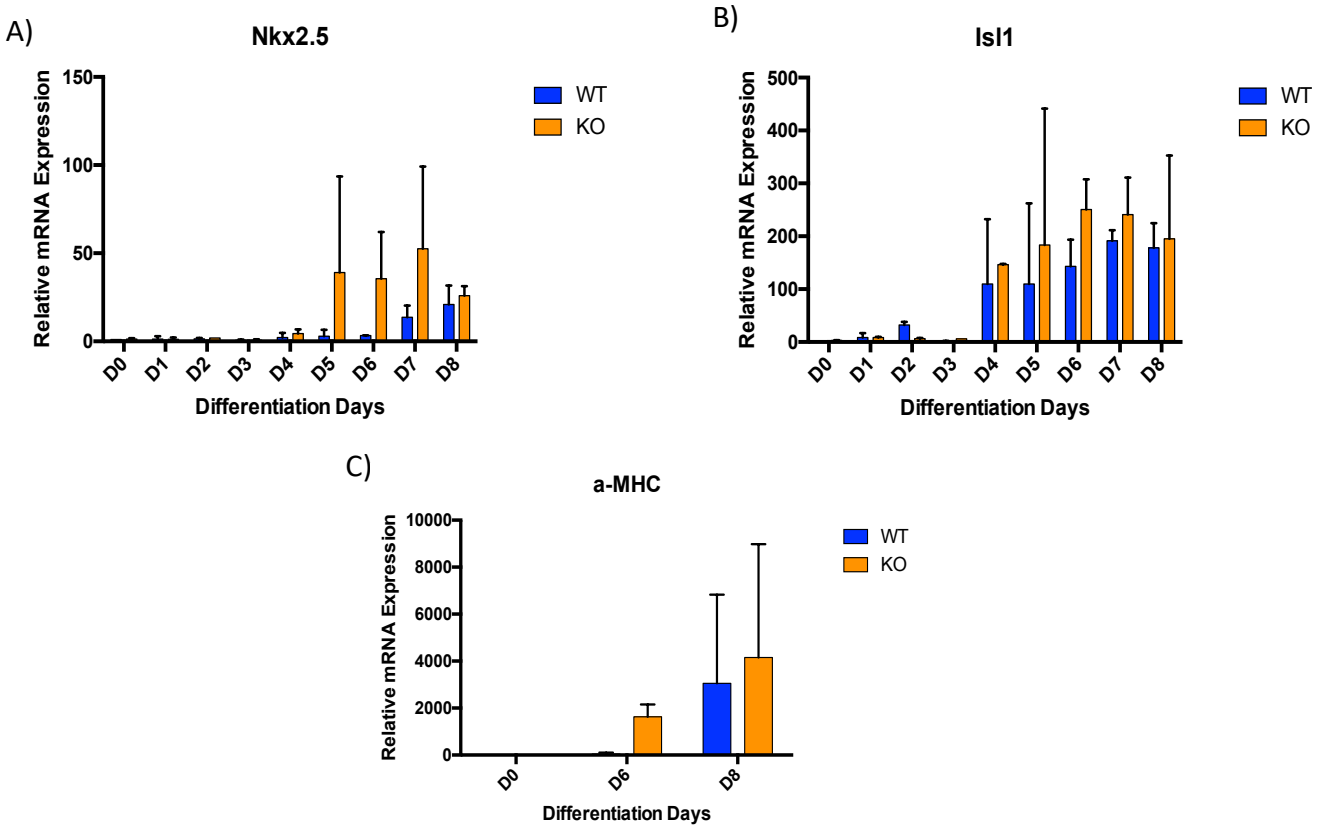

Figure 13 - ***Relative mRNA expression of cardiac genes in the WT and KO differentiated cells.***

qRT-PCR experiments were performed in triplicate for: (A) Nkx2.5; (B) Isl1; (C) α-MHC. α-MHC is only express after day 6 of differentiation so for this marker only day 6, 8 and 10 were tested. Results are represented as mean ± SD of two independent biological experiments. Two-Way ANOVA multiple comparisons Bonferroni test was applied to compare the differences between WT and KO groups in each day of differentiation. Statistically significant results were considered when *P<0.05; **P<0.01; ***P<0.001 and ****P<0.0001.

4.3. Pathways assessment

There are many important pathways involved in the development of the mouse heart, some of them have already been linked to *Cerl2*. It is known that *Cerl2* acts as an inhibitor of Nodal pathway during the break of symmetry in the node mouse (Marques et al., 2004). Nodal pathway is crucial for the L-R axis determination and for mesoderm and endoderm induction (Conlon et al., 1994). This signaling pathway is active when Nodal binds to its receptor, consequently phosphorylating Smad2 that will later form a complex with ρ-Smad4 and be able to translocate into the nucleus to activate Nodal's target genes, like *Pitx2* (Pauklin & Vallier, 2015). The Wnt/β-Catenin pathway is also essential for the heart development, this pathway is necessary for mesoderm induction and cardiac fate determination (Flaherty, Kamerzell, & Dawn, 2012). β-Catenin is actively being degraded by an Axin Complex that incorporates GSK3. When Wnt binds to its receptor the β-Catenin degradation stops, allowing its accumulation and translocation into the

nucleus where it will activate genes like Wnt3a (MacDonald, Tamai, & He, 2009). In 2014, Araújo et al. reported an increase of Nodal signaling the *Cerl2* KO neonatal mice hearts and unpublished work from the lab discovered an increase of Wnt signaling also in the *Cerl2* KO mice. Therefore, it was important to assess the activation of these two pathways in the *Cerl2* KO differentiated cells, in comparison with the WT ones. For this study, protein samples were extracted at each differentiation day and Western-Blots were performed using with anti-β-Catenin and anti-p-Smad2 antibodies (Table1 and Figure14). To correctly calculate the values of p-Smad2 it was also used a Smad2 antibody to measure the total levels of this protein. All the quantifications were normalized to a housekeeping gene – Tubulin. In figure 14A and B, it is possible to analyze and quantify the β-Catenin levels. Three independent differentiations were used but there was a lot of discrepancies in the β-Catenin level between the differentiations, resulting in high standard deviations. However, it is possible to see that there is an increase of β-Catenin at day 3, 4 and 5 in the *Cerl2* KO differentiated cells compared with the WT ones. The Western-Blots performed for both Smad2 and ρ-Smad2 did not work, due to unspecific bindings of the antibodies (Figure 14). Several optimizations were attempted, different concentrations of total protein, different antibody concentrations, as well as two different types of membranes – Nitrocellulose and PVDF, however, without success. One explanation for the unspecificity could be the polyclonal nature of this antibody, that recently became commercial unavailable. In the future, a monoclonal one should be tested.

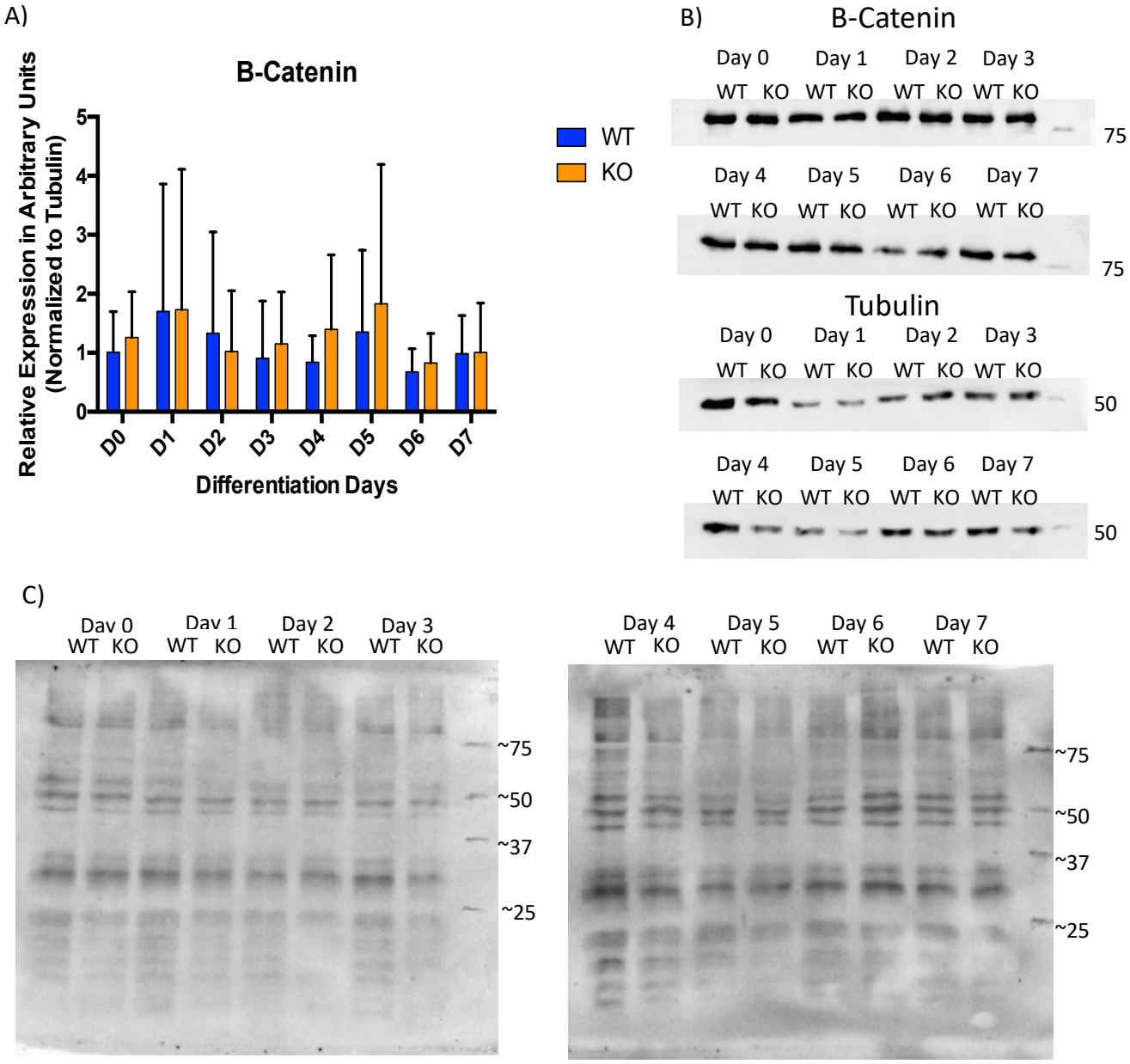

Figure 14 - ***Western-Blot results for B-Catenin and P-Smad2.***

Figure showing on (A) the quantification graph of western-blot results for β-Catenin from three independent differentiations. On (B) there is an example of the β-Catenin and Tubulin expression from the western-blot technique, used for quantification. β-Catenin is a 92kDa protein, so the bands appear slightly over the 75kDa mark and Tubulin is a 50kDa protein, showing its bands at the 50kDa mark. The panel (C) represents a membrane obtained from the western-blot technique and incubated for ρ-Smad2, showing unspecific binding.Two-Way ANOVA multiple comparisons Bonferroni test was applied to compare the differences between WT and KO groups in each day of differentiation. Statistically significant results were considered when *P<0.05; **P<0.01; ***P<0.001 and ****P<0.0001.

The assessment of the pathways was also performed by RT-PCR by analyzing the expression of target genes of both pathways – *Pitx2* for Nodal signaling and *Wnt3a* for Wnt signaling – and also by the expression of Nodal (that can activate itself) and β-Catenin (Figure 15). Once again, the reproducibility of the results was low and no statistical significance between WT and KO was observed. This could be explained by the lower number of differentiations analyzed. To get more

statistically significant data the number of experiments should be increase and better controlled as mention before. Nevertheless, it is possible to observe a trend on the *Pitx2* expression, which seems to be higher on the KO differentiated cells than on the WT ones (Figure 15A). On the *Wnt3a* expression pattern, there seems to be a shift in the peak of *Wnt3a* expression from day 4, on the WT samples, to day 3, on the KO (Figure 15B). Both *Nodal* and *β-Catenin* expression seem to peak one day before on the KO samples comparing with the WT (Figure 15C and D). On the *Cerl2* KO cells, the peak of expression of both genes is at day 2 of differentiation. β-Catenin presents a second upregulation where the expression of the WT cells seems to be higher than the expression of the KO ones (Figure 15D). The first upregulation of Nodal and β-Catenin apparently coincide with the mesoderm induction of the cardiac differentiation and these results may indicate that this induction happens earlier and with more expression on the KO differentiation which can explain the previous results of an earlier and higher expression of the cardiac progenitor markers.

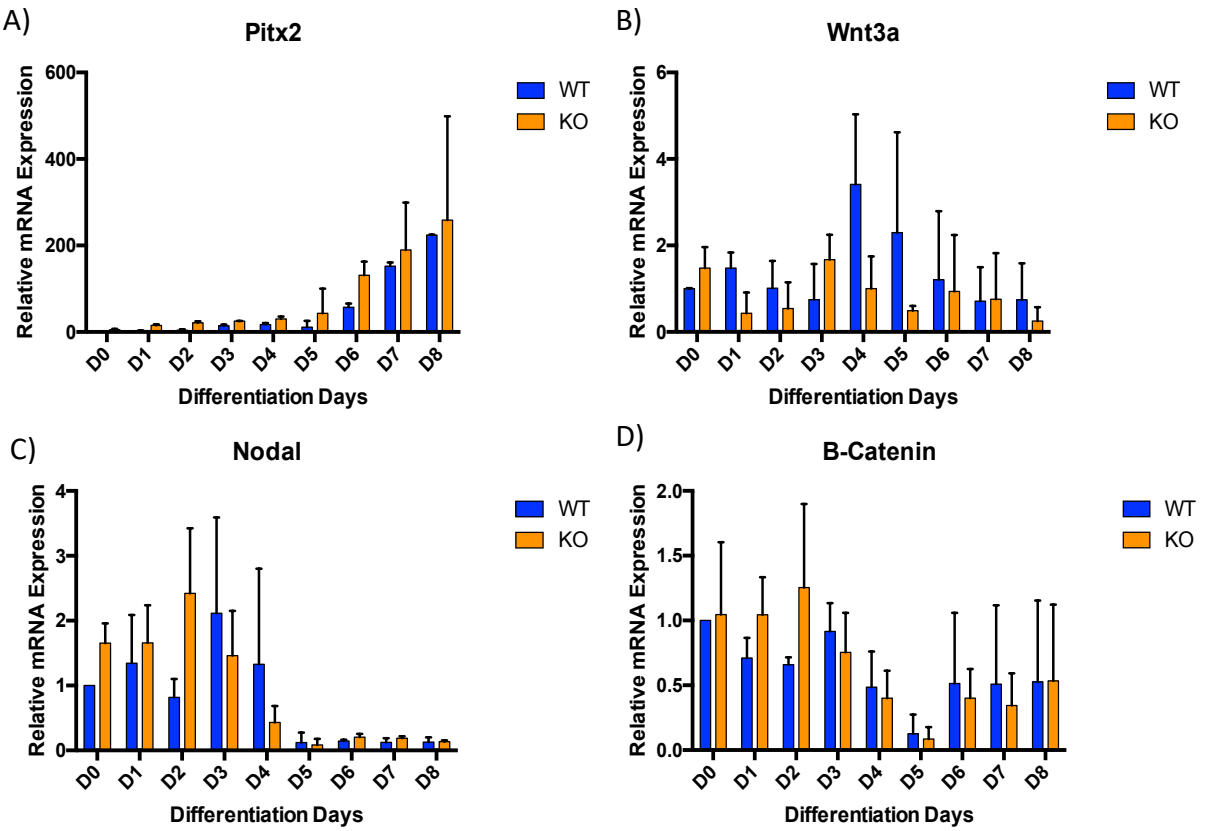

Figure 15 - ***Relative mRNA expression of downstream targets of Nodal and Wnt signaling pathways.***

qRT-PCR experiments were performed in triplicate for: (A) Pitx2; (B) Wnt3a; (C) Nodal; (D) β-Catenin. Results are represented as mean ± SD of two independent biological experiments. Two-Way ANOVA multiple comparisons Bonferroni test was applied to compare the differences between WT and KO groups in each day of differentiation. Statistically significant results were considered when *P<0.05; **P<0.01; ***P<0.001 and ****P<0.0001.

4.4. Differentiation Protocol with Activation of Nodal and Wnt Signaling Pathways

With the purpose of mimicking the *Cerl2* KO differentiation pattern in order to obtain a higher cardiomyocyte yield, a differentiation protocol was established considering the days of the pathways activation on the *Cerl2* KO differentiated cells. Activin is a member of the TGF-β superfamily of morphogens and its expressed in many different cell types at nearly all stages of development. Nodal and Activin mediated signaling are usually undistinguishable, as their ligands can regulate transcription by signaling through the same receptors and effectors, indicating that Activin can be used to activate Nodal signaling pathway (Pauklin & Vallier, 2015). The dose of Activin A (4ng/mL) necessary for the activation of Nodal signaling pathway in mouse embryonic stem cells was very well described elsewhere (Hartman et al., 2014). For the activation of the Wnt/β-Catenin signaling pathway, a highly specific and potent GSK3 inhibitor was used, by inhibiting GSK3, the degradation of β-Catenin is stopped, allowing its accumulation and consequent translocation into the nucleus (Chen et al., 2015). In literature, the dose of CHIR necessary for the activation of Wnt signaling pathway in mouse embryonic stem cells is more unclear. Therefore, as a first attempt for Wnt activation, a 10μM dose of CHIR99021 was used (Chen et al., 2015). This concentration revealed an unexpected phenotype where the cells, after being plated at day 5, did not expand and showed a peculiar morphology (Figure 16B). This unexpected phenotype was visible both when Activin A and CHIR99021 were used together (Figure 17A) and when only CHIR99021 was used (Figure 16B), indicating that the concentration of CHIR99021 had to be adjusted. For the remaining differentiations using CHIR99021 its concentration was adjusted to 5μM (Buikema et al., 2013). The expression of both Nodal and Wnt signaling pathways seem to reach its peak at day 3 on the KO cells (Figure 15B and C). From day 0 to day 2 of differentiation the cells are growing by the hanging drop method, making it difficult to add any substance to the medium, so the induction of Activin A and CHIR99021 to the medium started at day 2, when the plates return to its original state and new medium is added. The addition of the molecules was performed only in some plates and others were kept as a control (Figure 14A). For the differentiation where only, the Nodal pathway was activated (Figure 14B), Activin A was added to the medium at day 2 and 3 of differentiation, to sustain the activation of the pathway. The same protocol/activation protocol was performed for the differentiation where only the Wnt/β-Catenin pathway was activated. This long activation of Nodal did not express any significant differences in the morphology of the cells and neither on their ability to differentiate, when compared to the control ones. Both cell lines (No induction and W/ Induction 4ng/mL

Activin) started showing contractile movements at day 7/8 of differentiation (Figure 16B). On the other way, this long activation of Wnt signaling exhibited the previously discussed abnormal phenotype and the cells W/induction of 10µM CHIR99021 never showed contractile movements.

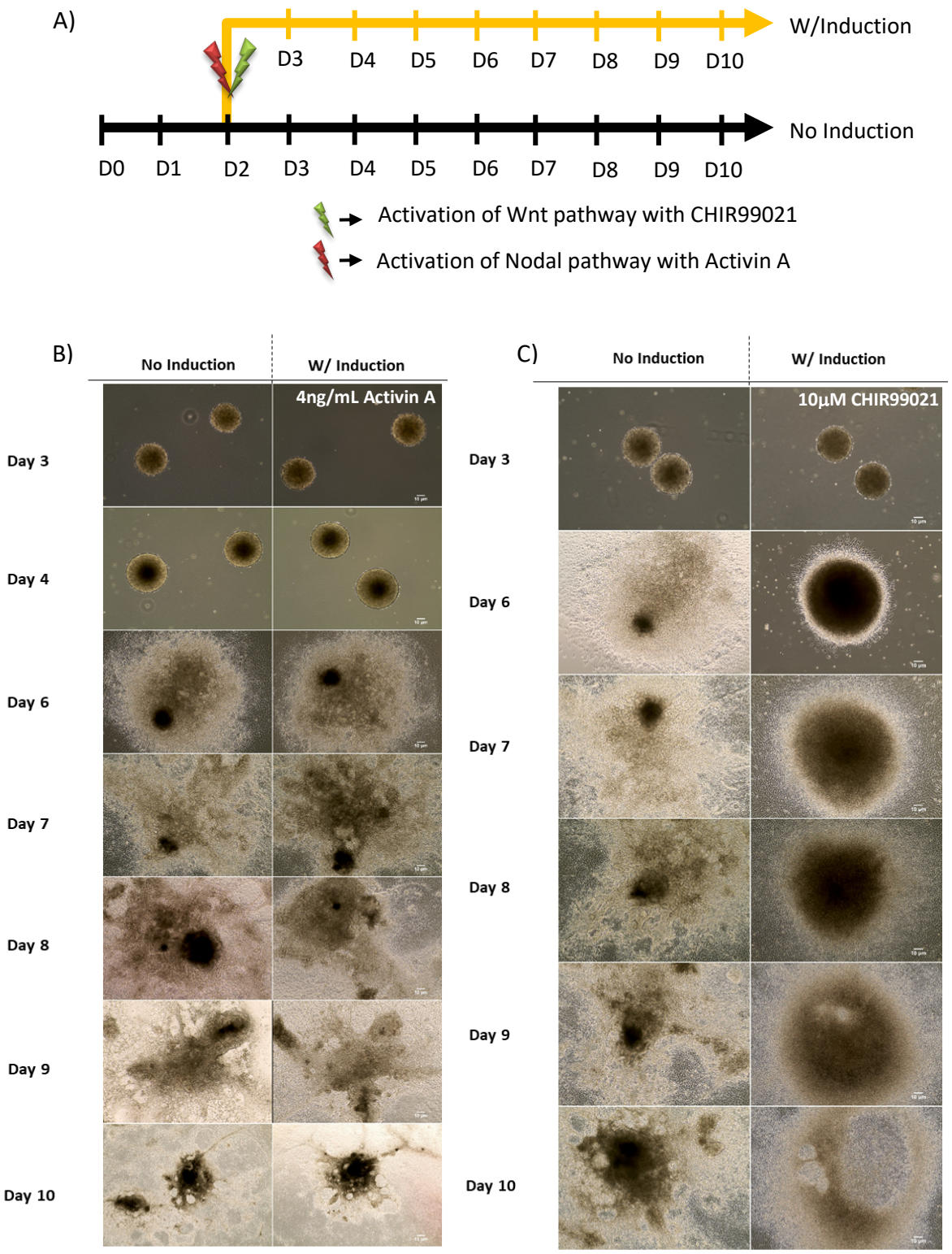

Figure 16 - ***Work plan for differentiation and morphology images of two differentiations at several differentiation***
The work flow of the experiments is represented at (A). On (B) the morphology of differentiated cells where Nodal was activated (W/Induction) did not show significant differences with the control (No Induction). On (C), where Wnt was activated (W/Induction)

there were no significant differences at day 3 but after day 6 it is notorious the differences between the two conditions. The EBs W/Induction did not expand from day 6 to 10 and showed an unexpected morphology. Scale bars: 10µm.

After validating that each pathway activated separately did not show the desired phenotype, as expected, new differentiations were performed activating Nodal and Wnt signaling pathways simultaneously. Similar to the previous differentiations, the activation of both pathways was initiated at day 2 of differentiation in some plates, while others were used as a control. In one differentiation it was used 4ng/mL of Activin and 10µM of CHIR99021 added at day 2 and 3 of differentiation to sustain the activation of the pathways. Comparable to what occurred on the differentiation where only Wnt was activated (Figure 16C), this differentiation with high levels of CHIR99021 and a long period of activation resulted in a similar phenotype observed in the previously mentioned differentiation (Figure 17A). At day 6 of differentiation (one day after the EBs were plated), the EBs W/ Induction (4ng/mL Activin A + 10µM CHIR99021) did not spread and exhibited an abnormal morphology, this unexpected phenotype was observed until day 10 of differentiation and they never showed contractile movements, contrasting with the No Induction cells that present a regular differentiation phenotype and also started showing contractile movements at day 7/8 (Figure 17A). The concentration of CHIR99021 was later adjusted to 5µM. Activin A and CHIR99021 were added only at day 2 of differentiation and 24H later the medium was extracted and new medium without molecules was added to plates, in order to prevent a longer activation of the pathways. The same procedure was performed on the control plates to avoid experimental discrepancies between the two conditions. With this experimental approach, at day 4 and 5 of differentiation the EBs with induction (4ng/mL Activin A + 5µM CHIR99021) appeared to be slightly bigger than the No Induction ones (Figure 17B), but measurements had to be performed in order to confirm this size difference. From day 6 to 10 there was no significant difference in the adhesion capacity and on the ability of the No Induction and W/Induction (4ng/mL Activin A + 5µM CHIR99021) EBs to expand on the plate. Interestingly, at day 6, the W/Induction (4ng/mL Activin A + 5µM CHIR99021) EBs started showing contractile movements in almost all of the plated EBs, while the No Induction ones only showed contractile movements at day 7/8 of differentiation. If the size of the W/ Induction EBs was confirmed to be larger than the No Induction ones, this could mean that there was an increase in the number of cells, after the activation of the pathways, as both cell lines started with the same number of cells per EB. It has been described that bigger EBs promote a better cardiac differentiation (Miyamoto & Nakazawa,

2016), which may explain why these EBs started showing contractile movements earlier than the No Induction differentiated cells.

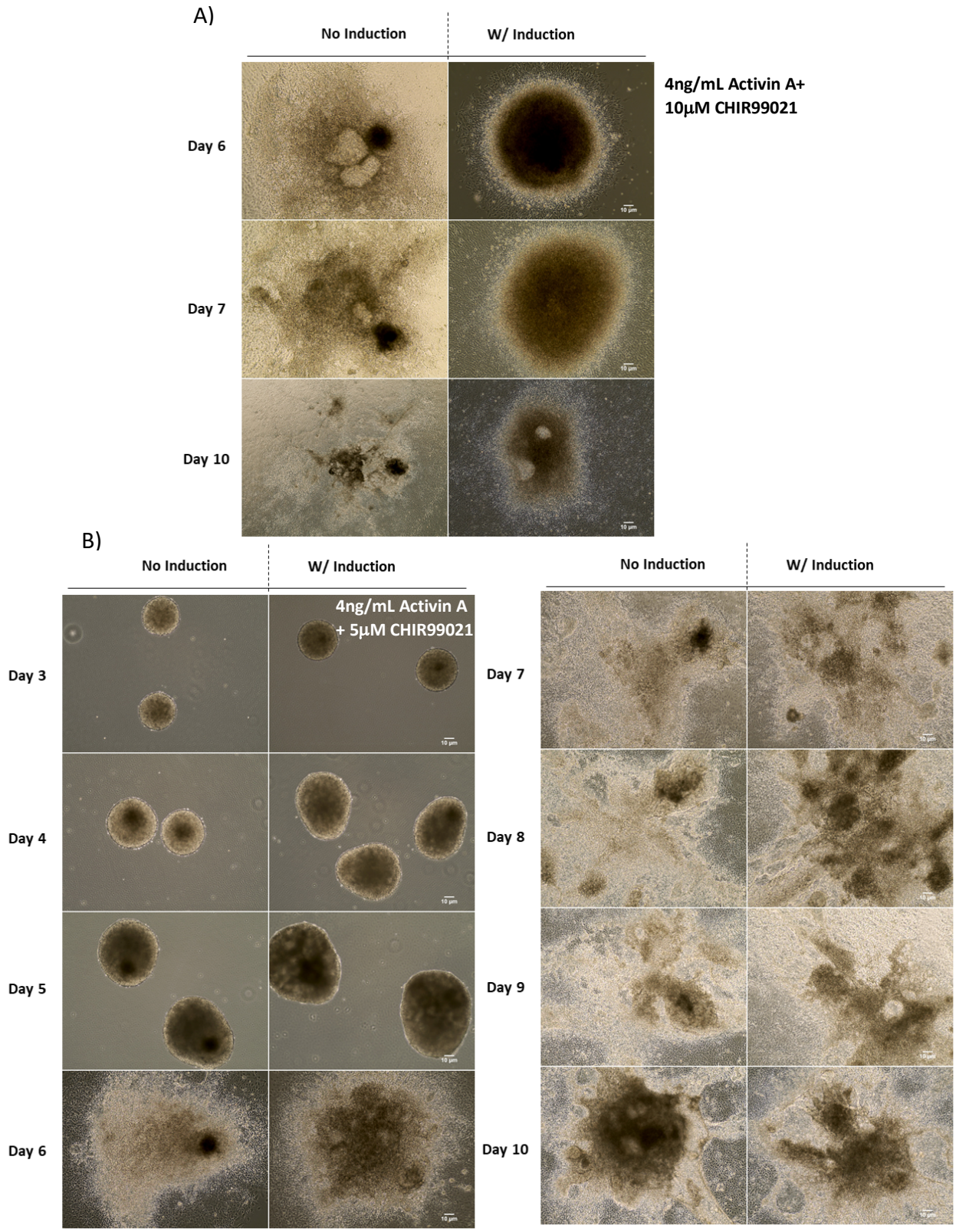

Figure 17 - ***Morphology images of two differentiations with activation of Wnt and Nodal signaling pathways simultaneously.*** The morphology of the EBs with the activation of the two pathways, using 4ng/mL of activin A and 10µM of CHIR99021 is represented in (A). It is notorious the differences between W/Induction and the control line. When the pathways were activated

using the previously mentioned concentrations, the EBs (W/Induction) did not expand and showed an unexpected morphology from day 6 to day 10. On (B) there is represented one differentiation using 4ng/mL and 5µM of CHIR99021 to activate both pathways. Some slightly differences are visible between the two conditions, like the size of the EBs at day 4 and 5 but further validation is needed to confirm this. Scale bars: 10µm.

In order to assess the phenotype of the W/Induction cells (4ng/mL Activin A + 5µM CHIR99021), the number of beating EBs were counted for day 6, 8 and 10 of differentiation and for each beating EB, the number of beating foci were also counted (Figure 18). For day 6 until day 9 of differentiation, 15 EBs were plated per day and per condition and for day 9 and 10 only 10 EBs were plated in the same conditions, these numbers could vary from 1 to 2 EBs per well. The EBs W/Induction started showing contractile movements at day 6 of differentiation, whereas the control did not show any contractile areas at this day, resulting in a statistically significant difference between the two conditions (Figure 18A). However, the number of beating foci per EB was significantly higher on the W/Induction cells, particularly at day 6 and 8 of differentiation (Figure 18B).

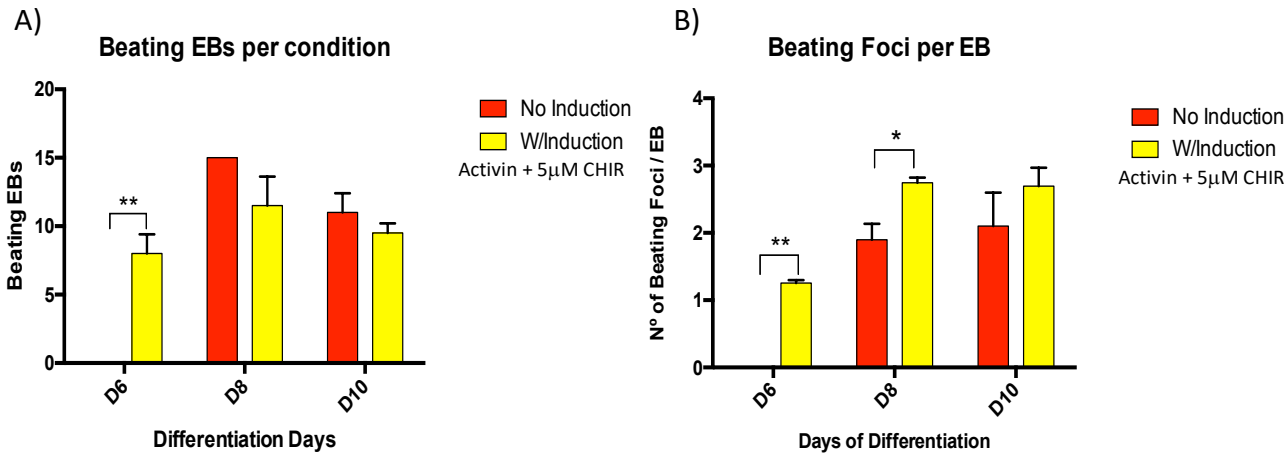

Figure 18 - ***Beating EBs per condition – No Induction (control) and W/Induction (Activin A and CHIR) and per EB.*** Results are expressed as the total number of beating foci with respect to the total number of plated EBs and represent the mean ± SD of two independent experiments. Two-Way ANOVA multiple comparisons Bonferroni test was applied to compare the differences between No Induction and W/Induction groups in each day of differentiation. Statistically significant results were considered when *P<0.05; **P<0.01; ***P<0.001 and ****P<0.0001.

4.5. Characterization of the modulated differentiations

The differentiations with the adjusted timepoints and concentrations of molecules, for the activation of Nodal and Wnt pathways simultaneously, seemed to show a similar phenotype to the one observed on the Cerl2 KO differentiated cells. So, the first thing to address on the differentiations with activation of Nodal and Wnt simultaneously was their activation and pattern of expression, to be compared with the results obtain for the *Cerl2* KO differentiated cells. By RT-PCR it was possible to observe an upregulation of *Pitx2* on the W/Induction condition (4ng/mL Activin A + 5µM CHIR99021), compared to the control (Figure 19A). This upregulation was

particularly evident at the days 7 and 8 of differentiation. Furthermore, these results presented a similar pattern of expression to the one produced by the *Cerl2* KO differentiated cells (Figure 15A and Figure 19A). *Wnt3a* showed a massive peak of expression, at day 3, on the W/Induction cells (4ng/mL Activin A + 5μM CHIR99021) meaning that the Wnt pathway was successfully activated at the correct timepoint (Figure 19B). However, when comparing the pattern of expression of the differentiation with activation of the pathways (Figure 19B) and the pattern of expression of the WT and *Cerl2* KO differentiation (Figure 15B), there are some differences to be addressed. On the WT and *Cerl2* KO differentiations, the KO cells showed a shift of the peak of expression of Wnt3a from day 4 (on the WT cells), to day 3 (on the KO cells), in fact the values of expression of Wnt3a on the KO cells were lower throughout the differentiation, except at day 3. The results obtained for Wnt3a of the manipulated differentiation (4ng/mL Activin A + 5μM CHIR99021) may support that the Wnt pathway was over-activated. Moreover, there was a visible decay of expression from day 3 to day 4 of differentiation, on the W/Induction cells (4ng/mL Activin A + 5μM CHIR99021), but after this decay the expression values were stabilized, whereas in the *Cerl2* KO cells, the *Wnt3a* expression the values continued their decay until day 5 and showed a slight increase at day 6. It will be necessary to further adjust the concentration of CHIR99021 in order to attain a more controlled activation of the Wnt pathway and possibly use a Wnt inhibitor, like IWP-4 that inhibits *Porcupine* expression, preventing the acylation of Wnt proteins needed to promote the binding of these proteins to the respective receptor (Tran & Zheng, 2017), in order to stop the Wnt pathway after day 3, getting an approximation to the *Cerl2* KO-like expression values. Interestingly, the *Nodal* expression at day 3 of differentiation was significantly lower on the W/Induction cells (4ng/mL Activin A + 5μM CHIR99021) comparable to the No Induction ones (Figure 19C). Since the *Pitx2* expression values indicate that the Nodal pathway was successfully activated, it is possible to hypothesize that some negative feedback was also activated at this day, inhibiting the *Nodal* expression at day 3. Nodal has several inhibitors and some of its downstream targets are those inhibitors, like *Lefty1/2*, meaning that Nodal is capable of activating a negative feedback mechanism for this pathway (Shen, 2007), so it would be enlightening to study the expression of some Nodal inhibitors that can be activated by Nodal itself. At day 2 of differentiation, there was no expression differences, for *Nodal*, between the two conditions (No induction and W/Induction by 4ng/mL Activin A + 5μM CHIR99021) (Figure 19C), contrasting to the results obtained for the WT and *Cerl2* KO differentiated cells, that presented a higher expression of *Nodal* on the KO cells at day 2 (Figure 15C), so possibly the activation of Nodal may have to be performed sooner. As

expected, the expression values of No Induction and W/Induction (4ng/mL Activin A + 5µM CHIR99021) for *β-Catenin* were very similar (Figure 19D). Since the pathway was activated by impairing the phosphorylation of β-Catenin, it was not expected to observe differences on the gene expression.

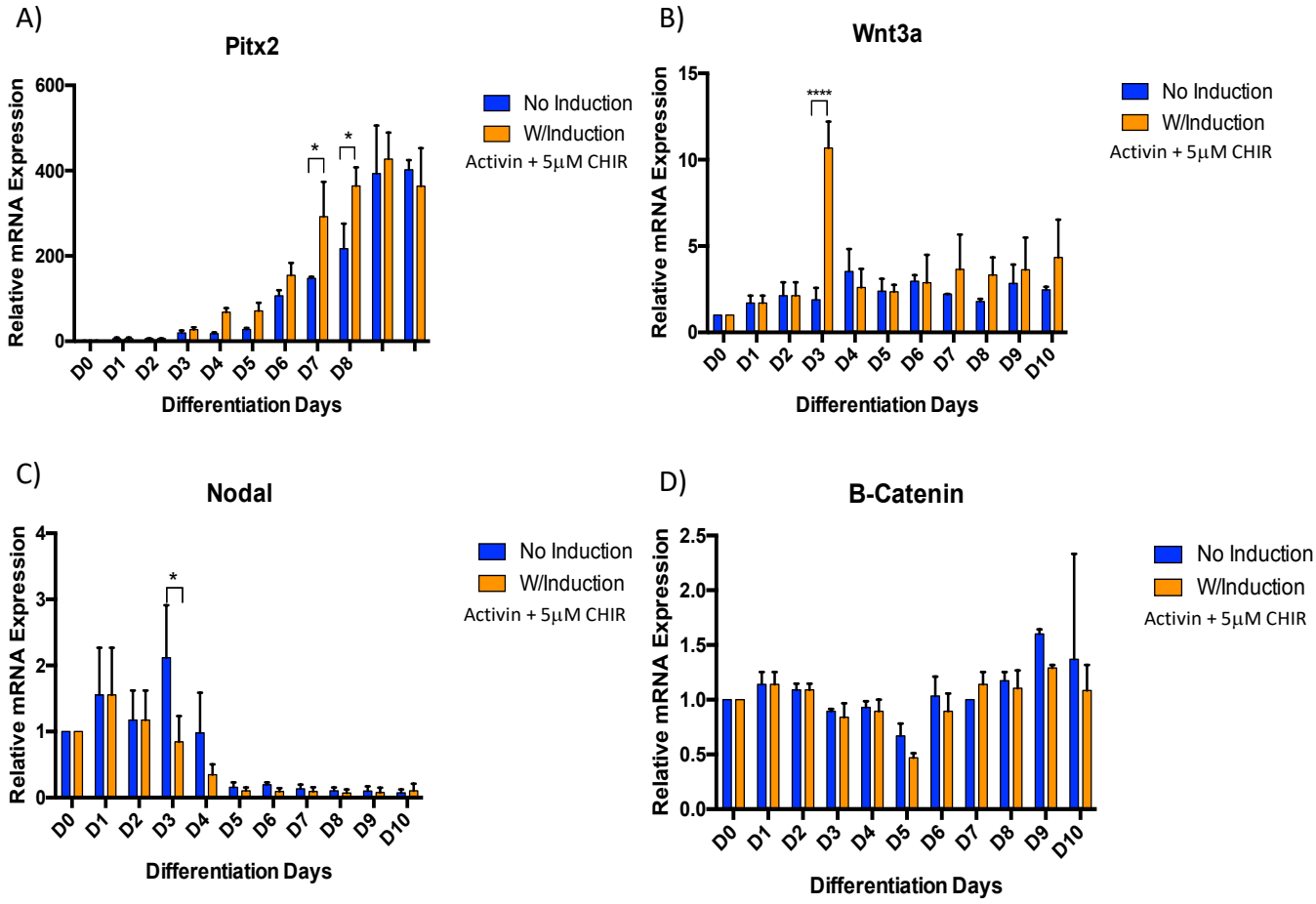

Figure 19 - ***Relative mRNA expression of downstream targets of Nodal and Wnt signaling pathways.***
qRT-PCR experiments of differentiations with modulation of Nodal and Wnt pathways simultaneously were performed in triplicate for: (A) Pitx2; (B) Wnt3a; (C) Nodal; (D) β-Catenin. Results are represented as mean ± SD of two independent biological experiments. Two-Way ANOVA multiple comparisons Bonferroni test was applied to compare the differences between WT and KO groups in each day of differentiation. Statistically significant results were considered when *P<0.05; **P<0.01; ***P<0.001 and ****P<0.0001.

The expression of Cerl2 was also measured and interestingly there was a notorious downregulation of this gene at day 4 on the W/Induction cells, yet they were still showing the second upregulation on day 9 that was also visible on the WT differentiated cells (Figure 20). Cerl2 usually peaks at day 4, during the first stages of cardiac differentiation, as explained previously, so the peak at day 4 on the No Induction cells was expected but its downregulation at the same day on the W/Induction cells (4ng/mL Activin A + 5µM CHIR99021) was unexpected. Nevertheless, this

downregulation at day 4 on the W/Induction cells (4ng/mL Activin A + 5µM CHIR99021) can possibly be explained by the activation of the Wnt pathway at day 3 of differentiation, since it is known that Wnt3 expression promotes Cerl2 mRNA decay (Nakamura et al., 2012).

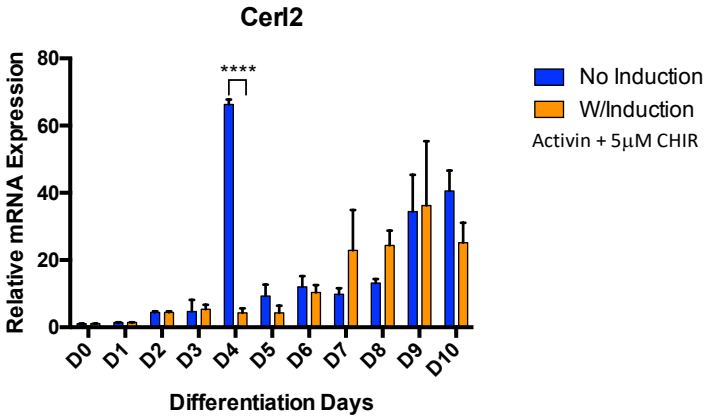

Figure 20 - ***Relative mRNA expression of Cerl2 in the No Induction cells compared to the W/Induction cells.***
qRT-PCR experiments of differentiations with modulation of Nodal and Wnt pathways simultaneously were performed in triplicate for Cerl2. Results are represented as mean ± SD of two independent biological experiments. Two-Way ANOVA multiple comparisons Bonferroni test was applied to compare the differences between WT and KO groups in each day of differentiation. Statistically significant results were considered when *P<0.05; **P<0.01; ***P<0.001 and ****P<0.0001.

Considering all the previous results, it was interesting to see that even though the phenotype of the differentiated cells W/Induction (4ng/mL Activin A + 5µM CHIR99021) was apparently similar to the phenotype expressed by the *Cerl2* KO cells, the patterns of expression of the several well-studied genes related to the Nodal and Wnt signaling pathways were not identical. In order to validate that the desired phenotype was really attained, the same cardiac markers previously studied for the WT and *Cerl2* KO differentiations were also assessed for the differentiations with modulation of the two pathways (Nodal and Wnt). It was visible that for all the markers studied (*Nkx2.5*, *Isl1* and *α-MHC*), the values of expression were not identical to the ones observed on the *Cerl2* KO cells (Figure 21 and Figure 13). The expression of *Nkx2.5* seem to appear sooner on the W/Induction (4ng/mL Activin A + 5µM CHIR99021) than on the control ones, with slightly higher expressions at day 4 and 5 of differentiation (Figure 21A). This upregulation is not sustained throughout the differentiation and the expression values of the No Induction cells surpass the expression values of the W/Induction cells (4ng/mL Activin A + 5µM CHIR99021), from day 6 to 10. *Isl1* also seems to be expressed earlier on the W/Induction cells (4ng/mL Activin A + 5µM CHIR99021) (day 4), comparing to the No Induction ones (day 5). The expression of *Isl1* was upregulated at day 3 and 4 of the W/Induction (4ng/mL Activin A + 5µM CHIR99021) cells but for the rest of the differentiation days (day 5 to 10) the expression o *Isl1* was significantly higher on the No Induction cells (Figure 21B). These two results suggest that the cardiac progenitors appear

earlier on the W/Induction cells (4ng/mL Activin A + 5μM CHIR99021) but do not necessarily exist at higher number for the rest of the differentiation on the W/Induction cells (4ng/mL Activin A + 5μM CHIR99021). The cardiomyocyte marker displayed the same evidence, *α-MHC* expression values were superior at day 6 on the W/Induction cells (4ng/mL Activin A + 5μM CHIR99021) but were later surpassed by the No Induction expression values at day 8 and 10 of differentiation. Taking all the results into account, it is evident that the *Cerl2* KO phenotype was not attained, so further manipulations on molecules concentrations and timepoints have to be tested.

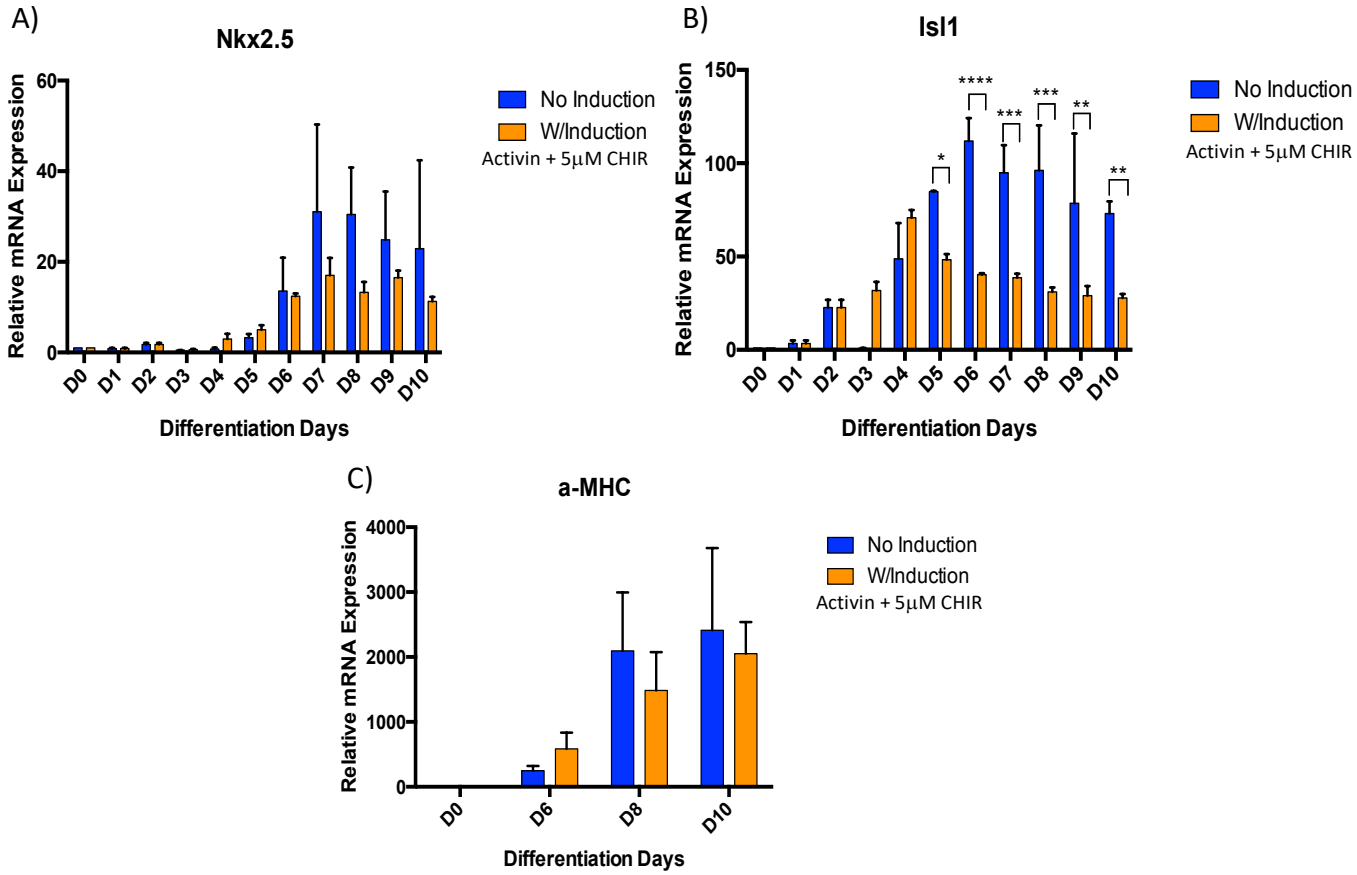

Figure 21 - ***Relative mRNA expression of cardiac genes in the WT and KO differentiated cells.***
qRT-PCR experiments were performed in triplicate for: (A) Nkx2.5; (B) Isl1; (C) α-MHC. α-MHC is only express after day 6 of differentiation so for this marker only day 6, 8 and 10 were tested. Results are represented as mean ± SD of two independent biological experiments. Two-Way ANOVA multiple comparisons Bonferroni test was applied to compare the differences between WT and KO groups in each day of differentiation. Statistically significant results were considered when *P<0.05; **P<0.01; ***P<0.001 and ****P<0.0001.

5. CONCLUSIONS AND FUTURE PRESPECTIVES

Mechanistic insights of the body functioning, as well as a better understanding of cellular and molecular mechanisms of disease may enable the development of treatments that are effective in broad patient populations. So, the use of stem cells as a model of disease has been a powerful tool to better understand those mechanisms. (Merkle & Eggan, 2013). With cardiac disease being responsible for 45% of all deaths in Europe, each year, and without available treatments except heart transplant on the late-stage of the disease, it has become an imperative to find alternative therapies to restore some quality of life to the patients (Timmis et al., 2019) (Nakanishi et al., 2016). Regenerative medicine has been one promising field in offering these patients a potential treatment, either as a cell-based therapy or by helping to better understand the disease, as well as, understanding the mechanisms underlying the heart development. Over the last decades, mutant ES have been used as disease models to study specificities and uncover the biological mechanisms that lead to the origin of congenital heart diseases, through the generation of cardiomyocytes by differentiating those cells (Dambrot et al., 2011)

The *Cerl2* gene, member of the Cerberus/Dan family is an important protein for the L-R axis establishment by working as an inhibitor of Nodal, thus regulating its expression (Marques et al., 2014) When loss-of-function of *Cerl2* is verified, the resulted mutant phenotype is described by, not only congenital laterality disorders but also for congenital heart defects, independent of the laterality defects. It has been described and increase in the left ventricular myocardium wall and systolic disfunction, motivated by cardiomyocyte hyperplasia. Upon further analysis to these hearts, it was described an upregulation of both Nodal and Wnt signaling pathways (Marques et al., 2014) (Araújo et al., 2014).

In the present dissertation, with the purpose of uncover the role of Cerl2 in controlling these two specific signaling pathways – Nodal signaling and Wnt signaling – WT and *Cerl2* KO ES cell lines were characterized for the activation patterns of the two previously mentioned pathways. The hypothesis that both Nodal and Wnt signaling pathways are upregulated in the Cerl2 KO cells might explain the high number of *Cerl2* KO stem cells-derived cardiomyocytes observed during spontaneous differentiation, which also correlates to the phenotype described by Araújo (2014) and her colleagues in the neonatal mouse hearts.

Here, by RT-PCR, it is demonstrated that *Pitx2* (downstream target of Nodal) showed an upregulation trend throughout the spontaneous differentiation of the KO cells, whereas Wnt3a (downstream target of Wnt) showed a shift on the expression peak from day 4, observed on the

WT cells, to day 3 on the KO ones. Nodal and β-Catenin also showed a shift on their activation peak from day 3 (WT cells) to day 2 (KO cells). Moreover, it was observed that *Cerl2* KO cells, usually started showing contractile movements sooner than the WT ones, and exhibiting also more beating foci per EB. In addition, the cardiac markers – *Nkx2.5*; *Isl1*; *α-MHC* – were upregulated on the *Cerl2* KO differentiated cells, being Nkx2.5 and α-MHC expressed earlier on the *Cerl2* KO then on the WT differentiated ones. Taking together, this data may indicate an earlier and more preeminent cardiac mesoderm induction as a result of an earlier and higher activation of both Nodal and Wnt signaling pathways on the Cerl2 KO cells. Also, the upregulation of Nkx2.5, at day 5 of differentiation, might result on a high number of FHF progenitors that could explain the enlarged myocardium of the left ventricle's walls observed in the Cerl2 KO mice.

To further validate the importance of Nodal and Wnt signaling pathways for the *Cerl2* KO differentiation outcome, in this work, several differentiations were performed testing the single and the co-activation of both Nodal and Wnt signaling pathways. The co-activation of both Nodal and Wnt signaling pathways showed a similar phenotype to the one observed for the *Cerl2* KO spontaneous differentiation, displaying contractile movements at day 6, sooner than the control cells and presenting also a higher number of beating foci per EB than the control line. Curiously, the expression level of the cardiac markers *Nkx2.5*, *Isl1*, and *α-MHC* is relatively lower, for almost all the tested differentiation days, on the +Activin/+CHIR differentiation when compared to the control. However, *Isl1* showed higher expression levels at days 3 and 4 and *α-MHC* was also higher at day 6 on the +Activin/+CHIR differentiation, meaning that cardiac progenitors and later cardiomyocytes are developing sooner but not necessarily in a higher number. Furthermore, the activation of the pathways did not display a similar pattern to the one exhibited by the *Cerl2* KO cells. It is possible that the Wnt signaling pathway activation was too strong, impairing a necessary downregulation after reaching its peak. Even though the *Pitx2* expression values were similar to the *Cerl2* KO differentiation, the levels of Nodal were lower, especially at day 3, which can possible indicate that some negative feedback control was activated upon the activation of the pathway. Interestingly, *Cerl2* presented a high downregulation of its expression. A previous study reported feedback loops interlinking the Wnt signaling pathway and Cerl2 capable to generate together the L-R asymmetry at the mouse node and revealed the capacity of Cerl2 in inhibition of the Wnt self-activating loop, with Wnt3a inhibiting Cerl2 (Nakamura et al., 2012). It is visible that the major downregulation of *Cerl2* occurs at day 4, one day after *Wnt3a* reached its peak, this can possibly indicate that *Wnt3a* may be suppressing *Cerl2* after activation of the Wnt pathway.

As a future work, several concentrations of Activin A and CHIR99021 have to be used with their induction at different timepoints, in order to understand if the *Cerl2* KO phenotype is achieved by the manipulation of Nodal and Wnt signaling pathways. This will provide further information on the role of *Cerl2* in regulating these two pathways. On the other hand, it is crucial to analyze, the differentiated *Cerl2* KO ES cell populations, as well as the modulated ones, using Flow Cytometry experiments. With this technique it is possible to have a reliable quantitative result related to the number of derived cardiac progenitor cells and cardiomyocytes of all the conditions, which can be also important to understand if the higher number of beating foci observed on the W/Induction differentiation was correlated to a higher number of cardiomyocytes. In addition, it will be relevant to perform proliferation assays to assess the proliferation capacity of the *Cerl2* KO and manipulated derived- cardiomyocytes by performing a BrdU labelling assay.

BIBLIOGRAPHY

Araújo, A., Marques, S. and Belo, J. (2014). Targeted Inactivation of Cerberus Like-2 Leads to Left Ventricular Cardiac Hyperplasia and Systolic Dysfunction in the Mouse. *PLoS ONE*, 9(7), p.e102716

Artus, J., Piliszek, A., & Hadjantonakis, A.-K. (2011). The primitive endoderm lineage of the mouse blastocyst: Sequential transcription factor activation and regulation of differentiation by Sox17. *Developmental Biology*, *350*(2), 393–404. https://doi.org/10.1016/j.ydbio.2010.12.007

Beddington, R. S., & Robertson, E. J. (1999). Axis Development and Early Asymmetry in Mammals. *Cell*, *96*(2), 195–209. https://doi.org/10.1016/s0092-8674(00)80560-7

Bedzhov, I., Graham, S. J. L., Leung, C. Y., & Zernicka-Goetz, M. (2014). Developmental plasticity, cell fate specification and morphogenesis in the early mouse embryo. *Philosophical Transactions of the Royal Society B: Biological Sciences*, *369*(1657), 20130538. https://doi.org/10.1098/rstb.2013.0538

Belo, J., Marques, S. and Inácio, J. (2017). The Role of Cerl2 in the Establishment of Left-Right Asymmetries during Axis Formation and Heart Development. *Journal of Cardiovascular Development and Disease*, 4(4), p.23.

Belo, J., Silva, A. C., Borges, A. C., Filipe, M., Bento, M., Gonalves, L., … Marques, S. (2009). Generating asymmetries in the early vertebrate embryo: the role of the Cerberus-like family. *The International Journal of Developmental Biology*, *53*(8-9–10), 1399–1407. Retrieved from https://www.academia.edu/18429137/Generating_asymmetries_in_the_early_vertebrate_embryo_the_role_of_the_Cerberus-like_family

Borowiak, M., Maehr, R., Chen, S., Chen, A., Tang, W., Fox, J., Schreiber, S. and Melton, D. (2009). Small Molecules Efficiently Direct Endodermal Differentiation of Mouse and Human Embryonic Stem Cells. *Cell Stem Cell*, 4(4), pp.348-358.

Boulton, J., Henry, R., Roddick, L. G., Rogers, D., Thompson, L. and Warner, G. (1991). Survival after neonatal myocardial infarction. *Pediatrics,* 88, pp.145-150.

Bouwmeester, T., Kim, S.-H., Sasai, Y., Lu, B., & Robertis, E. M. D. (1996). Cerberus is a head-inducing secreted factor expressed in the anterior endoderm of Spemann's organizer. *Nature*, *382*(6592), 595–601. https://doi.org/10.1038/382595a0

Bruneau, B. G. (2002). Transcriptional regulation of vertebrate cardiac morphogenesis. *Circulation Research*, *90*(5), 509–519. https://doi.org/10.1161/01.res.0000013072.51957.b7

Buikema, J. W., Mady, A. S., Mittal, N. V., Atmanli, A., Caron, L., Doevendans, P. A., … Domian, I. J. (2013). Wnt/ -catenin signaling directs the regional expansion of first and second heart field-derived ventricular cardiomyocytes. *Development*, *140*(20), 4165–4176. https://doi.org/10.1242/dev.099325

Bustin, S. (2000). Absolute quantification of mRNA using real-time reverse transcription polymerase chain reaction assays. *Journal of Molecular Endocrinology*, 169–193. https://doi.org/10.1677/jme.0.0250169

Cai, W., Guzzo, R. M., Wei, K., Willems, E., Davidovics, H., & Mercola, M. (2012). A Nodal-to-TGFβ Cascade Exerts Biphasic Control Over Cardiopoiesis. *Circulation Research*, *111*(7), 876–881. https://doi.org/10.1161/circresaha.112.270272

Cambria, E., Steiger, J., Günter, J., Bopp, A., Wolint, P., Hoerstrup, S. P., & Emmert, M. Y. (2016). Cardiac Regenerative Medicine: The Potential of a New Generation of Stem Cells. *Transfusion Medicine and Hemotherapy*, *43*(4), 275–281. https://doi.org/10.1159/000448179

Chadwick Jayaraj, J., Davatyan, K., Subramanian, S. S., & Priya, J. (2019). Epidemiology of Myocardial Infarction. *Myocardial Infarction*. https://doi.org/10.5772/intechopen.74768

Chan, M. M., Smith, Z. D., Grosswendt, S., Kretzmer, H., Norman, T. M., Adamson, B., … Weissman, J. S. (2002). Molecular recording of mammalian embryogenesis. *Nature*, *570*(7759), 77–82. https://doi.org/10.1038/s41586-019-1184-5

Chen, Y., Zeng, D., Ding, L., Li, X.-L., Liu, X.-T., Li, W.-J., … Zheng, Q.-S. (2015). Three-dimensional poly-(ε-caprolactone) nanofibrous scaffolds directly promote the cardiomyocyte differentiation of murine-induced pluripotent stem cells through Wnt/β-catenin signaling. *BMC Cell Biology*, *16*(1). https://doi.org/10.1186/s12860-015-0067-3

Choi, J., Huebner, A. J., Clement, K., Walsh, R. M., Savol, A., Lin, K., … Hochedlinger, K. (2017). Prolonged Mek1/2 suppression impairs the developmental potential of embryonic stem cells. *Nature*, *548*(7666), 219–223. https://doi.org/10.1038/nature23274

Conlon, F., Lyons, K., Takaesu, N., Barth, K., Kispert, A., Herrmann, B., & Robertson, E. (1994). A primary requirement for nodal in the formation and maintenance of the primitive streak in the mouse. *Development*, *120*(7), 1919–1928. Retrieved from https://dev.biologists.org/content/develop/120/7/1919.full.pdf

Cristo, F., Inácio, J. M., de Almeida, S., Mendes, P., Martins, D. S., Maio, J., … Belo, J. A. (2017). Functional study of DAND5 variant in patients with Congenital Heart Disease and laterality defects. *BMC Medical Genetics*, *18*(1). https://doi.org/10.1186/s12881-017-0444-1

Czubryt, M. (2012). Common threads in cardiac fibrosis, infarct scar formation, and wound healing. *Fibrogenesis & Tissue Repair*. http://www.fibrogenesis.com/content/5/1/19

Dambrot, C., Passier, R., Atsma, D., & Mummery, C. L. (2011). Cardiomyocyte differentiation of pluripotent stem cells and their use as cardiac disease models. *Biochemical Journal*, *434*(1), 25–35. https://doi.org/10.1042/bj20101707

Davidson, B. P., & Tam, P. P. L. (2000). The node of the mouse embryo. *Current Biology*, *10*(17), R617–R619. https://doi.org/10.1016/s0960-9822(00)00675-8

Desgrange, A., Le Garrec, J.-F., & Meilhac, S. M. (2018). Left-right asymmetry in heart development and disease: forming the right loop. *Development*, *145*(22), dev162776. https://doi.org/10.1242/dev.162776

Doetschman, T. C., Harald Eistetter, Katz, M., Schmidt, W., & Kemler, R. (1985). The in vitro development of blastocyst-derived embryonic stem cell lines: formation of visceral yolk sac, blood islands and myocardium. *Development*, *87*(1), 27–45. Retrieved from https://dev.biologists.org/content/87/1/27.long

Evans, M. J., & Kaufman, M. H. (1981). Establishment in culture of pluripotential cells from mouse embryos. *Nature*, *292*(5819), 154–156. https://doi.org/10.1038/292154a0

Fan, Y., Ho, B. X., Pang, J. K. S., Pek, N. M. Q., Hor, J. H., Ng, S.-Y., & Soh, B.-S. (2018). Wnt/β-catenin-mediated signaling re-activates proliferation of matured cardiomyocytes. *Stem Cell Research & Therapy*, *9*(1). https://doi.org/10.1186/s13287-018-1086-8

Fischer, K. M., Cottage, C. T., Wu, W., Din, S., Gude, N. A., Avitabile, D., … Sussman, M. A. (2009). Enhancement of Myocardial Regeneration Through Genetic Engineering of Cardiac Progenitor Cells Expressing Pim-1 Kinase. *Circulation*, *120*(21), 2077–2087. https://doi.org/10.1161/circulationaha.109.884403

Flaherty, M. P., Kamerzell, T. J., & Dawn, B. (2012). Wnt Signaling and Cardiac Differentiation. *Progress in Molecular Biology and Translational Science*, *11*, 153–174. https://doi.org/10.1016/b978-0-12-398459-3.00007-1

Galdos, F. X., Guo, Y., Paige, S. L., VanDusen, N. J., Wu, S. M., & Pu, W. T. (2017). Cardiac Regeneration. *Circulation Research*, *120*(6), 941–959. https://doi.org/10.1161/circresaha.116.309040

Grabarek, J. B., Zyzynska, K., Saiz, N., Piliszek, A., Frankenberg, S., Nichols, J., … Plusa, B. (2011). Differential plasticity of epiblast and primitive endoderm precursors within the ICM of the early mouse embryo. *Development*, *139*(1), 129–139. https://doi.org/10.1242/dev.067702

Guzman-Ayala, M., Lee, K. L., Mavrakis, K. J., Goggolidou, P., Norris, D. P., & Episkopou, V. (2009). Graded Smad2/3 Activation Is Converted Directly into Levels of Target Gene Expression in Embryonic Stem Cells. *PLoS ONE*, *4*(1), e4268. https://doi.org/10.1371/journal.pone.0004268

Hamada, H., Meno, C., Watanabe, D., & Saijoh, Y. (2002). Establishment of vertebrate left–right asymmetry. *Nature Reviews Genetics*, *3*(2), 103–113. https://doi.org/10.1038/nrg732

Hanna, J., Markoulaki, S., Mitalipova, M., Cheng, A. W., Cassady, J. P., Staerk, J., … Jaenisch, R. (2009). Metastable Pluripotent States in NOD-Mouse-Derived ESCs. *Cell Stem Cell*, *4*(6), 513–524. https://doi.org/10.1016/j.stem.2009.04.015

Hartman, M. E., Librande, J. R., Medvedev, I. O., Ahmad, R. N., Moussavi-Harami, F., Gupta, P. P., … Chin, M. T. (2014). An Optimized and Simplified System of Mouse Embryonic Stem Cell Cardiac

Differentiation for the Assessment of Differentiation Modifiers. *PLoS ONE*, *9*(3), e93033. https://doi.org/10.1371/journal.pone.0093033

Haubner, B. J., Schneider, J., Schweigmann, U., Schuetz, T., Dichtl, W., Velik-Salchner, C., … Penninger, J. M. (2016). Functional Recovery of a Human Neonatal Heart After Severe Myocardial Infarction. *Circulation Research*, *118*(2), 216–221. https://doi.org/10.1161/circresaha.115.307017

Icardo, J. M., García Rincón, J. M., & Ángeles Ros, M. (2002). Congenital Heart Disease, Heterotaxia and Laterality. *Revista Española de Cardiología (English Version)*, *55*(9), 962–974. https://doi.org/10.1016/s0300-8932(02)76735-3

Ieda, M., Fu, J.-D., Delgado-Olguin, P., Vedantham, V., Hayashi, Y., Bruneau, B. G., & Srivastava, D. (2010). Direct Reprogramming of Fibroblasts into Functional Cardiomyocytes by Defined Factors. *Cell*, *142*(3), 375–386. https://doi.org/10.1016/j.cell.2010.07.002

Inácio, J. M., Marques, S., Nakamura, T., Shinohara, K., Meno, C., Hamada, H., & Belo, J. A. (2013). The Dynamic Right-to-Left Translocation of Cerl2 Is Involved in the Regulation and Termination of Nodal Activity in the Mouse Node. *PLoS ONE*, *8*(3), e60406. https://doi.org/10.1371/journal.pone.0060406

Ivanovitch, K., Esteban, I., & Torres, M. (2017). Growth and Morphogenesis during Early Heart Development in Amniotes. *Journal of Cardiovascular Development and Disease*, *4*(4), 20. https://doi.org/10.3390/jcdd4040020

Komiya, Y., & Habas, R. (2008). Wnt signal transduction pathways. *Organogenesis*, *4*(2), 68–75. https://doi.org/10.4161/org.4.2.5851

Kurosawa, H. (2007). Methods for inducing embryoid body formation: in vitro differentiation system of embryonic stem cells. *Journal of Bioscience and Bioengineering*, *103*(5), 389–398. https://doi.org/10.1263/jbb.103.389

Le Bin, G. C., Munoz-Descalzo, S., Kurowski, A., Leitch, H., Lou, X., Mansfield, W., … Nichols, J. (2014). Oct4 is required for lineage priming in the developing inner cell mass of the mouse blastocyst. *Development*, *141*(5), 1001–1010. https://doi.org/10.1242/dev.096875

Leitolis, A., Robert, A. W., Pereira, I. T., Correa, A., & Stimamiglio, M. A. (2019). Cardiomyogenesis Modeling Using Pluripotent Stem Cells: The Role of Microenvironmental Signaling. *Frontiers in Cell and Developmental Biology*, *7*. https://doi.org/10.3389/fcell.2019.00164

Li, X., Chen, Y., Schéele, S., Arman, E., Haffner-Krausz, R., Ekblom, P., & Lonai, P. (2001). Fibroblast Growth Factor Signaling and Basement Membrane Assembly Are Connected during Epithelial Morphogenesis of the Embryoid Body. *The Journal of Cell Biology*, *153*(4), 811–822. https://doi.org/10.1083/jcb.153.4.811

Lin, C.-J., Lin, C.-Y., Chen, C.-H., Zhou, B., & Chang, C.-P. (2012). Partitioning the heart: mechanisms of cardiac septation and valve development. *Development*, *139*(18), 3277–3299. https://doi.org/10.1242/dev.063495

MacDonald, B. T., Tamai, K., & He, X. (2009). Wnt/β-Catenin Signaling: Components, Mechanisms, and Diseases. *Developmental Cell*, *17*(1), 9–26. https://doi.org/10.1016/j.devcel.2009.06.016

Malaguti, M., Nistor, P. A., Blin, G., Pegg, A., Zhou, X., & Lowell, S. (2013). Bone morphogenic protein signalling suppresses differentiation of pluripotent cells by maintaining expression of E-Cadherin. *ELife*, *2*. https://doi.org/10.7554/elife.01197

Maltsev, V., Rohwedel, J., Hescheler, J., & Wobus, A. (1993). Embryonic stem cells differentiate in vitro into cardiomyocytes representing sinusnodal, atrial and ventricular cell types. *Mechanisms of Development*, *44*(1), 41–50. https://doi.org/10.1016/0925-4773(93)90015-p

Marques, S., Borges, A., Silva, A., Freitas, S., Cordenonsi, M., & Belo, J. (2004). The activity of the Nodal antagonist Cerl-2 in the mouse node is required for correct L/R body axis. *Genes & Development*, *18*(19), 2342–2347. https://doi.org/10.1101/gad.306504

Martin, G. R. (1981). Isolation of a pluripotent cell line from early mouse embryos cultured in medium conditioned by teratocarcinoma stem cells. *Proceedings of the National Academy of Sciences*, *78*(12), 7634–7638. https://doi.org/10.1073/pnas.78.12.7634

Matsuo, I., & Hiramatsu, R. (2017). Mechanical perspectives on the anterior-posterior axis polarization of mouse implanted embryos. *Mechanisms of Development*, *144*, 62–70. https://doi.org/10.1016/j.mod.2016.09.002

Mehta, A., Ramachandra, C. J. A., Sequiera, G. L., Sudibyo, Y., Nandihalli, M., Yong, P. J. A., … Shim, W. (2014). Phasic modulation of Wnt signaling enhances cardiac differentiation in human pluripotent stem cells by recapitulating developmental ontogeny. *Biochimica et Biophysica Acta (BBA) - Molecular Cell Research*, *1843*(11), 2394–2402. https://doi.org/10.1016/j.bbamcr.2014.06.011

Meilhac, S. M., Lescroart, F., Blanpain, C., & Buckingham, M. E. (2014). Cardiac Cell Lineages that Form the Heart. *Cold Spring Harbor Perspectives in Medicine*, *4*(9), a013888–a013888. https://doi.org/10.1101/cshperspect.a013888

Merkle, F. T., & Eggan, K. (2013). Modeling Human Disease with Pluripotent Stem Cells: from Genome Association to Function. *Cell Stem Cell*, *12*(6), 656–668. https://doi.org/10.1016/j.stem.2013.05.016

Miyamoto, D., & Nakazawa, K. (2016). Differentiation of mouse iPS cells is dependent on embryoid body size in microwell chip culture. *Journal of Bioscience and Bioengineering*, *122*(4), 507–512. https://doi.org/10.1016/j.jbiosc.2016.03.018

Molkentin, J. (1996). α-myosin Heavy Chain Gene Regulation: Delineation and Characterization of the Cardiac Muscle-specific Enhancer and Muscle-specific Promoter. *Journal of Molecular and Cellular Cardiology*, *28*(6), 1211–1225. https://doi.org/10.1006/jmcc.1996.0112

Moorman, A., Webb, S., Brown, N. A., Lamers, W., & Anderson, R. H. (2003). Development Of The Heart: (1) Formation Of The Cardiac Chambers And Arterial Trunks. *Heart*, *89*(7), 806–814. https://doi.org/10.1136/heart.89.7.806

Morris, S. A., Grewal, S., Barrios, F., Patankar, S. N., Strauss, B., Buttery, L., … Zernicka-Goetz, M. (2012). Dynamics of anterior–posterior axis formation in the developing mouse embryo. *Nature Communications*, *3*(1). https://doi.org/10.1038/ncomms1671

Nakamura, T., Mine, N., Nakaguchi, E., Mochizuki, A., Yamamoto, M., Yashiro, K., … Hamada, H. (2006). Generation of Robust Left-Right Asymmetry in the Mouse Embryo Requires a Self-Enhancement and Lateral-Inhibition System. *Developmental Cell*, *11*(4), 495–504. https://doi.org/10.1016/j.devcel.2006.08.002

Nakamura, T., Saito, D., Kawasumi, A., Shinohara, K., Asai, Y., Takaoka, K., … Hamada, H. (2012). Fluid flow and interlinked feedback loops establish left–right asymmetric decay of Cerl2 mRNA. *Nature Communications*, *3*(1). https://doi.org/10.1038/ncomms2319

Nishioka, N., Inoue, K., Adachi, K., Kiyonari, H., Ota, M., Ralston, A., … Sasaki, H. (2009). The Hippo Signaling Pathway Components Lats and Yap Pattern Tead4 Activity to Distinguish Mouse Trophectoderm from Inner Cell Mass. *Developmental Cell*, *16*(3), 398–410. https://doi.org/10.1016/j.devcel.2009.02.003

Niwa, H., Ogawa, K., Shimosato, D., & Adachi, K. (2009). A parallel circuit of LIF signalling pathways maintains pluripotency of mouse ES cells. *Nature*, *460*(7251), 118–122. https://doi.org/10.1038/nature08113

Niwa, H., Toyooka, Y., Shimosato, D., Strumpf, D., Takahashi, K., Yagi, R., & Rossant, J. (2005). Interaction between Oct3/4 and Cdx2 Determines Trophectoderm Differentiation. *Cell*, *123*(5), 917–929. https://doi.org/10.1016/j.cell.2005.08.040

Nonaka, S., Shiratori, H., Saijoh, Y., & Hamada, H. (2002). Determination of left–right patterning of the mouse embryo by artificial nodal flow. *Nature*, *418*(6893), 96–99. https://doi.org/10.1038/nature00849

Oki, S., Hashimoto, R., Okui, Y., Shen, M. M., Mekada, E., Otani, H., … Hamada, H. (2007). Sulfated glycosaminoglycans are necessary for Nodal signal transmission from the node to the left lateral plate in the mouse embryo. *Development*, *134*(21), 3893–3904. https://doi.org/10.1242/dev.009464

Pauklin, S., & Vallier, L. (2015). Activin/Nodal signalling in stem cells. *Development*, *142*(4), 607–619. https://doi.org/10.1242/dev.091769

Piccolo, S., Agius, E., Leyns, L., Bhattacharyya, S., Grunz, H., Bouwmeester, T., & Robertis, E. M. D. (1999). The head inducer Cerberus is a multifunctional antagonist of Nodal, BMP and Wnt signals. *Nature*, *397*(6721), 707–710. https://doi.org/10.1038/17820

Qian, L., Huang, Y., Spencer, C. I., Foley, A., Vedantham, V., Liu, L., … Srivastava, D. (2012). In vivo reprogramming of murine cardiac fibroblasts into induced cardiomyocytes. *Nature*, *485*(7400), 593–598. https://doi.org/10.1038/nature11044

Ramsdell, A. F. (2005). Left–right asymmetry and congenital cardiac defects: Getting to the heart of the matter in vertebrate left–right axis determination. *Developmental Biology*, *288*(1), 1–20. https://doi.org/10.1016/j.ydbio.2005.07.038

Robertson, E. J. (1987). *Teratocarcinomas and embryonic stem cells a pract. approach*. Oxford [U.A.] Irl Pr.

Rungarunlert, S. (2009). Embryoid body formation from embryonic and induced pluripotent stem cells: Benefits of bioreactors. *World Journal of Stem Cells*, *1*(1), 11. https://doi.org/10.4252/wjsc.v1.i1.11

Saga, Y., Hata, N., Kobayashi, S., Magnuson, T., Seldin, M. F., & Taketo, M. M. (1996). MesP1: a novel basic helix-loop-helix protein expressed in the nascent mesodermal cells during mouse gastrulation. *Development (Cambridge, England)*, *122*(9), 2769–2778. Retrieved from https://www.ncbi.nlm.nih.gov/pubmed/8787751

Samuel, L. J., & Latinkić, B. V. (2009). Early Activation of FGF and Nodal Pathways Mediates Cardiac Specification Independently of Wnt/β-Catenin Signaling. *PLoS ONE*, *4*(10), e7650. https://doi.org/10.1371/journal.pone.0007650

Sasaki, H. (2015). Position- and polarity-dependent Hippo signaling regulates cell fates in preimplantation mouse embryos. *Seminars in Cell & Developmental Biology*, *47–48*, 80–87. https://doi.org/10.1016/j.semcdb.2015.05.003

Savolainen, S. M., Foley, J. F., & Elmore, S. A. (2009). Histology Atlas of the Developing Mouse Heart with Emphasis on E11.5 to E18.5. *Toxicologic Pathology*, *37*(4), 395–414. https://doi.org/10.1177/0192623309335060

Shen, M. M. (2007). Nodal signaling: developmental roles and regulation. *Development*, *134*(6), 1023–1034. https://doi.org/10.1242/dev.000166

Shioi, G., Hoshino, H., Abe, T., Kiyonari, H., Nakao, K., Meng, W., … Aizawa, S. (2017). Apical constriction in distal visceral endoderm cells initiates global, collective cell rearrangement in embryonic visceral endoderm to form anterior visceral endoderm. *Developmental Biology*, *429*(1), 20–30. https://doi.org/10.1016/j.ydbio.2017.07.004

Shiratori, H., & Hamada, H. (2006). The left-right axis in the mouse: from origin to morphology. *Development*, *133*(11), 2095–2104. https://doi.org/10.1242/dev.02384

Smith, A. G., Heath, J. K., Donaldson, D. D., Wong, G. G., Moreau, J., Stahl, M., & Rogers, D. (1988). Inhibition of pluripotential embryonic stem cell differentiation by purified polypeptides. *Nature*, *336*(6200), 688–690. https://doi.org/10.1038/336688a0

Srivastava, D. (2016). Reprogramming Approaches to Cardiovascular Disease: From Developmental Biology to Regenerative Medicine. *Etiology and Morphogenesis of Congenital Heart Disease*, 3–10. https://doi.org/10.1007/978-4-431-54628-3_1

Strumpf, D. (2005). Cdx2 is required for correct cell fate specification and differentiation of trophectoderm in the mouse blastocyst. *Development*, *132*(9), 2093–2102. https://doi.org/10.1242/dev.01801

Tai, C.-I., & Ying, Q.-L. (2013). Gbx2, a LIF/Stat3 target, promotes reprogramming to and retention of the pluripotent ground state. *Journal of Cell Science*, *126*(5), 1093–1098. https://doi.org/10.1242/jcs.118273

Taylor, D. A., Atkins, B. Z., Hungspreugs, P., Jones, T. R., Reedy, M. C., Hutcheson, K. A., … Kraus, W. E. (1998). *Regenerating functional myocardium: Improved performance after skeletal myoblast transplantation*. *Nature Medicine*, *4*(8), 929–933. https://doi.org/10.1038/nm0898-929

Timmis, A., Townsend, N., Gale, C., Grobbee, R., Maniadakis, N., Flather, M., … Logstrup, S. (2017). European Society of Cardiology: Cardiovascular Disease Statistics 2017. *European Heart Journal*, *39*(7), 508–579. https://doi.org/10.1093/eurheartj/ehx628

Tran, F. H., & Zheng, J. J. (2017). Modulating the wnt signaling pathway with small molecules. *Protein Science*, *26*(4), 650–661. https://doi.org/10.1002/pro.3122

Vincent, S. D., & Buckingham, M. E. (2010). How to Make a Heart. *Organogenesis in Development*, *90*, 1–41. https://doi.org/10.1016/s0070-2153(10)90001-x

Voges, H. K., Mills, R. J., Elliott, D. A., Parton, R. G., Porrello, E. R., & Hudson, J. E. (2017). Development of a human cardiac organoid injury model reveals innate regenerative potential. *Development*, *144*(6), 1118–1127. https://doi.org/10.1242/dev.143966

Weitzer, G. (2006). Embryonic stem cell-derived embryoid bodies: an in vitro model of eutherian pregastrulation development and early gastrulation. *Handbook of Experimental Pharmacology*, (174), 21–51. Retrieved from https://www.ncbi.nlm.nih.gov/pubmed/16370323

Williams, M., Burdsal, C., Periasamy, A., Lewandoski, M., & Sutherland, A. (2011). Mouse primitive streak forms in situ by initiation of epithelial to mesenchymal transition without migration of a cell population. *Developmental Dynamics*, *241*(2), 270–283. https://doi.org/10.1002/dvdy.23711

Williams, M., Burdsal, C., Periasamy, A., Lewandoski, M., & Sutherland, A. (2011). Mouse primitive streak forms in situ by initiation of epithelial to mesenchymal transition without migration of a cell population. *Developmental Dynamics*, *241*(2), 270–283. https://doi.org/10.1002/dvdy.2371

Wilson, P., D'Agostino, R., Levy, D., Belanger, A., Silbershatz, H., & Kannel, W. (1998). *Prediction of Coronary Heart Disease Using Risk Factor Categories.* Circulation. https://doi.org/10.1161/01.CIR.97.18.1837

Xin, M., Olson, E. N., & Bassel-Duby, R. (2013). Mending broken hearts: cardiac development as a basis for adult heart regeneration and repair. *Nature Reviews Molecular Cell Biology*, *14*(8), 529–541. https://doi.org/10.1038/nrm3619

Ying, Q.-L., Nichols, J., Chambers, I., & Smith, A. (2003). BMP Induction of Id Proteins Suppresses Differentiation and Sustains Embryonic Stem Cell Self-Renewal in Collaboration with STAT3. *Cell*, *115*(3), 281–292. https://doi.org/10.1016/s0092-8674(03)00847-x

Ying, Q.-L., Wray, J., Nichols, J., Batlle-Morera, L., Doble, B., Woodgett, J., … Smith, A. (2008). The ground state of embryonic stem cell self-renewal. *Nature*, *453*(7194), 519–523. https://doi.org/10.1038/nature06968

Yu, J. K., Franceschi, W., Huang, Q., Pashakhanloo, F., Boyle, P. M., & Trayanova, N. A. (2019). A comprehensive, multiscale framework for evaluation of arrhythmias arising from cell therapy in the whole post-myocardial infarcted heart. *Scientific Reports*, *9*(1). https://doi.org/10.1038/s41598-019-45684-0